Please provide feedback

Please support the ScholarWorks@UMBC repository by emailing scholarworks-group@umbc.edu and telling us what having access to this work means to you and why it's important to you. Thank you.

Atmospheric
Chemistry
and Physics

Decadal changes in summertime reactive oxidized nitrogen and surface ozone over the Southeast United States

Jingyi Li[1], **Jingqiu Mao**[2], **Arlene M. Fiore**[3], **Ronald C. Cohen**[4,5], **John D. Crounse**[6], **Alex P. Teng**[6],
Paul O. Wennberg[6,7], **Ben H. Lee**[8], **Felipe D. Lopez-Hilfiker**[8], **Joel A. Thornton**[8], **Jeff Peischl**[9,10], **Ilana B. Pollack**[11],
Thomas B. Ryerson[9], **Patrick Veres**[9,10], **James M. Roberts**[9], **J. Andrew Neuman**[9,10], **John B. Nowak**[12,a],
Glenn M. Wolfe[13,14], **Thomas F. Hanisco**[14], **Alan Fried**[15], **Hanwant B. Singh**[16], **Jack Dibb**[17], **Fabien Paulot**[18,19], **and**
Larry W. Horowitz[19]

[1]Jiangsu Key Laboratory of Atmospheric Environment Monitoring and Pollution Control, Collaborative Innovation Center of Atmospheric Environment and Equipment Technology, School of Environmental Science and Engineering, Nanjing University of Information Science and Technology, Nanjing 210044, China
[2]Department of Chemistry and Biochemistry & Geophysical Institute, University of Alaska Fairbanks, Fairbanks, AK 99775, USA
[3]Department of Earth and Environmental Sciences & Lamont-Doherty Earth Observatory of Columbia University, Palisades, NY 10964, USA
[4]Department of Chemistry, University of California, Berkeley, Berkeley, CA 94720, USA
[5]Department of Earth and Planetary Science, University of California, Berkeley, Berkeley, CA 94720, USA
[6]Division of Geological and Planetary Sciences, California Institute of Technology, Pasadena, CA 91125, USA
[7]Division of Engineering and Applied Science, California Institute of Technology, Pasadena, CA 91125, USA
[8]Department of Atmospheric Sciences, University of Washington, Seattle, WA 98195, USA
[9]Chemical Sciences Division, NOAA Earth System Research Laboratory, Boulder, CO 80305, USA
[10]Cooperative Institute for Research in Environmental Science, University of Colorado Boulder, Boulder, CO 80309, USA
[11]Department of Atmospheric Science, Colorado State University, Fort Collins, CO 80523, USA
[12]Aerodyne Research, Inc., Billerica, MA 01821, USA
[13]Joint Center for Earth System Technology, University of Maryland Baltimore County, Baltimore, MD 21250, USA
[14]Atmospheric Chemistry and Dynamics Lab, NASA Goddard Space Flight Center, Greenbelt, MD 20771, USA
[15]Institute of Arctic & Alpine Research, University of Colorado Boulder, Boulder, CO 80309, USA
[16]NASA Ames Research Center, Moffett Field, CA 94035, USA
[17]Department of Earth Sciences and Institute for the Study of Earth, Oceans, and Space, University of New Hampshire, Durham, NH 03824, USA
[18]Program in Atmospheric and Oceanic Sciences, Princeton University, Princeton, NJ 08544, USA
[19]Geophysical Fluid Dynamics Laboratory/National Oceanic and Atmospheric Administration, Princeton, NJ 08540, USA
[a]now at: NASA Langley Research Center, Hampton, VA 23681, USA

Correspondence: Jingqiu Mao (jmao2@alaska.edu)

Abstract. Widespread efforts to abate ozone (O_3) smog have significantly reduced emissions of nitrogen oxides (NO_x) over the past 2 decades in the Southeast US, a place heavily influenced by both anthropogenic and biogenic emissions. How reactive nitrogen speciation responds to the reduction in NO_x emissions in this region remains to be elucidated. Here we exploit aircraft measurements from ICARTT (July–August 2004), SENEX (June–July 2013), and SEAC^{4}RS (August–September 2013) and long-term ground measurement networks alongside a global chemistry–climate model to examine decadal changes in summertime reactive oxidized nitrogen (RON) and ozone over the Southeast US. We show that our model can reproduce the mean vertical profiles of major RON species and the total (NO_y) in both 2004 and 2013. Among the major RON species, nitric acid (HNO_3) is dominant (~ 42–45%), followed by NO_x (31%), total peroxy nitrates (ΣPNs; 14%), and total alkyl nitrates (ΣANs; 9–12%) on a regional scale. We find that most RON species, including NO_x, ΣPNs, and HNO_3, decline proportionally with decreasing NO_x emissions in this region, leading to a similar decline in NO_y. This linear response might be in part due to the nearly constant summertime supply of biogenic VOC emissions in this region. Our model captures the observed relative change in RON and surface ozone from 2004 to 2013. Model sensitivity tests indicate that further reductions of NO_x emissions will lead to a continued decline in surface ozone and less frequent high-ozone events.

1 Introduction

Since the 1990s, the US Environmental Protection Agency (US EPA) has targeted emissions of nitrogen oxides (NO_x) to improve air quality by lowering regional photochemical smog (the 1990 Clean Air Amendment). Satellite- and ground-based observations imply significant declines in US NO_x emissions, with a decreasing rate of roughly $-4\% \, yr^{-1}$ after 2005 (Krotkov et al., 2016; Russell et al., 2012; Tong et al., 2015; Miyazaki et al., 2017; Lu et al., 2015; Lamsal et al., 2015). This has proven effective at lowering near-surface ozone (O_3) in the past few decades (Cooper et al., 2012; Simon et al., 2015; Hidy and Blanchard, 2015; Stoeckenius et al., 2015; Xing et al., 2015; Yahya et al., 2016; Astitha et al., 2017). The average of the annual fourth highest daily maximum 8 h average (MDA8) ozone over 206 sites has decreased by 31 % from 101 ppb in 1980 to 70 ppb in 2016 across the continental US, with more significant reductions in rural areas of the eastern US in summer (Simon et al., 2015; Cooper et al., 2012). Here we use both aircraft- and ground-based datasets, combined with a high-resolution chemistry–climate model, to evaluate responses of reactive oxidized nitrogen (RON) and surface ozone to the NO_x emission reductions in the Southeast US.

In the troposphere, ozone is produced through photochemical reactions involving NO_x and volatile organic compounds (VOCs) in the presence of sunlight. During photooxidation, a large fraction of NO_x is transformed into its reservoirs, including nitric acid (HNO_3), peroxy nitrates (RO_2NO_2; dominated by peroxyacetyl nitrate, or PAN), and alkyl nitrates ($RONO_2$). These species, together with NO_x, are known as total reactive oxidized nitrogen ($NO_y = NO_x + HNO_3 + HONO + 2 \times N_2O_5 +$ total peroxy nitrates, or ΣPNs + total alkyl nitrates, or ΣANs). Some of these reservoir species, particularly those with an organic component, tend to be less soluble and longer lived. They may carry reactive nitrogen far from the NO_x source region (Stohl et al., 2002; Parrish et al., 2004; Li et al., 2004) and thereby affect NO_x concentrations and ozone formation on a regional to global scale (Liang et al., 1998; Horowitz et al., 1998; Perring et al., 2013; Paulot et al., 2016; Hudman et al., 2004).

$RONO_2$ originating from biogenic VOCs (BVOCs) represents a major uncertainty in the NO_y budget, as BVOC emissions account for more than 80 % of global VOC emissions (Millet et al., 2008). To a large extent, this is due to uncertainties in the current understanding of BVOC oxidation chemistry. Biogenic $RONO_2$ species are mainly produced from the oxidation of BVOCs by OH in the presence of NO_x during daytime and by the nitrate radical (NO_3) during nighttime. Laboratory and field studies show a wide range of $RONO_2$ yields from their BVOC precursors (Browne et al., 2014; Fry et al., 2014; Lockwood et al., 2010; Paulot et al., 2009; Rindelaub et al., 2015; Rollins et al., 2009; Lee et al., 2014; Xiong et al., 2015, 2016; Teng et al., 2015). Another uncertainty lies in the fate of $RONO_2$; i.e., recycling $RONO_2$ into NO_x or converting it to HNO_3 has important implications for the NO_y budget and thus ozone production (Fiore et al., 2005; Horowitz et al., 2007; Ito et al., 2009; Perring et al., 2013; Paulot et al., 2012). This is further complicated by particle-phase $RONO_2$, an important component of secondary organic aerosol (SOA) over the Southeast US (Xu et al., 2015; Lee et al., 2016). The fate of particle-phase $RONO_2$ is unclear, with the possibility for removal by hydrolysis to form HNO_3 (Jacobs et al., 2014; Hu et al., 2011; Darer et al., 2011; Rindelaub et al., 2015; Szmigielski et al., 2010; Sato, 2008; Romer et al., 2016; Wolfe et al., 2015; Boyd et al., 2015, 2017; Bean and Hildebrandt Ruiz, 2016), photochemical aging (Nah et al., 2016), and deposition (Nguyen et al., 2015). To what extent $RONO_2$ affects the partitioning of RON and surface ozone remains to be elucidated.

Extensive datasets in the Southeast US offer a great opportunity to study the decadal changes in RON and surface ozone resulting from NO_x emission decline. Aircraft campaigns during the summers of 2004 and 2013, including the International Consortium for Atmospheric Research on Transport and Transformation (ICARTT; Fehsenfeld et al., 2006; Singh et al., 2006), the Southeast Nexus (SENEX; Warneke et al., 2016), and the Studies of Emissions and Atmospheric Composition, Clouds and Climate Coupling by

Regional Surveys (SEAC[4]RS; Toon et al., 2016), provide detailed characterization of tropospheric composition in this region separated by nearly a decade. These data have been widely used to evaluate model estimates of RON and ozone (Singh et al., 2007; Pierce et al., 2007; Perring et al., 2009; Fischer et al., 2014; Hudman et al., 2007; Henderson et al., 2011; Hudman et al., 2009; Edwards et al., 2017; Baker and Woody, 2017; Travis et al., 2016; Mao et al., 2013b; Fisher et al., 2016; Yu et al., 2016; Liu et al., 2016). Together with measurements from surface networks, including the National Atmospheric Deposition Program (NADP) and EPA Air Quality System (AQS), these datasets enable a close examination of responses of RON and surface ozone to NO_x emission reductions in this region.

Here we use a high-resolution global 3-D chemistry–climate model, the Geophysical Fluid Dynamics Laboratory (GFDL) AM3 model with updated isoprene and organic nitrate chemistry, to investigate decadal changes in summertime RON and surface ozone between 2004 and 2013 over the Southeast US. We first evaluate the model with comprehensive measurements from three aircraft campaigns in the summers of 2004 (ICARTT) and 2013 (SENEX and SEAC[4]RS). Model estimates of nitrate wet deposition flux are also evaluated against measurements from NADP; model estimates of NO_y are compared with measurements from EPA AQS to provide an additional constraint on the fate of RON in the model. We then investigate the repartitioning of RON in response to NO_x emission reductions from 2004 to 2013 on a regional scale. From there, we examine model estimates of decadal changes in summertime surface ozone at 157 EPA AQS monitoring sites over the Southeast US. We also demonstrate the sensitivity of RON and MDA8 ozone to a hypothetical NO_x emission reduction over the next decade.

2 Methodology

2.1 AM3 Model

We apply a high-resolution ($50 \times 50\,km^2$) version of the GFDL AM3 global chemistry–climate model to study decadal changes in RON and ozone over the Southeast US. Chemistry–climate models provide a unique capability to both evaluate model representation of these observed changes and use that to improve future projections of air quality in the same region. The model configuration is to a large extent similar to that used in another paper (Li et al., 2016) and a short summary is provided below. The dynamical core, physical parameterizations, cloud and precipitation processes, and cloud–aerosol interactions mainly follow Donner et al. (2011), except that convective plumes are computed on a vertical grid with finer resolution (Paulot et al., 2016). Dry deposition in the model has been updated to use dry deposition velocities calculated in the GEOS-Chem model (Paulot et al., 2016) to reflect the rapid deposition of organic nitrates

and oxidized volatile organic compounds (OVOCs; Nguyen et al., 2015). The current time step for chemistry and transport in our model is 20 min. We show below in Sect. 3.1 that with the current setting our model can reproduce the vertical profiles of RON. The sensitivity of RON to operator duration can be found in Philip et al. (2016).

Isoprene emissions are computed in the model using the Model of Emissions of Gases and Aerosols from Nature (MEGAN). In 2004, isoprene emissions over the continental US (25–50° N, 130–70° W) are computed to be 8.0 Tg C in July and August together, with a previous model estimate of 7.5 Tg C by Mao et al. (2013b). In 2013, model estimates of isoprene emissions were scaled down by 20 % following Li et al. (2016). The resulting isoprene emissions are 7.7 Tg C in July–August in this region, with little difference compared to 2004. Monoterpene emissions follow Naik et al. (2013) and do not vary interannually, with a total of 4.0 Tg C in July and August.

Anthropogenic emissions follow the Representative Concentration Pathway 8.5 (RCP8.5) projection (Lamarque et al., 2011) for both 2004 and 2013 to compare the model to observations in a consistent fashion and also enable the future projection of air quality in this region. As shown in Table 1, anthropogenic NO_x emissions over the continental US during July–August 2004 amount to $0.42\,Tg\,N\,month^{-1}$, which is consistent with Hudman et al. (2007) but 11 % lower than the EPA estimate of $0.47\,Tg\,N\,month^{-1}$ (Granier et al., 2011). For the year 2013, we apply a 25 % reduction to anthropogenic NO_x emissions from the RCP8.5 projection (from base year of 2010) to best reproduce the vertical profiles of RON during SENEX as shown below in Sect. 3.1. This adjustment is also consistent with recent estimates of NO_x emissions over the Southeast US (Anderson et al., 2014). The resulting anthropogenic NO_x emissions ($0.25\,Tg\,N\,month^{-1}$) are 14 % lower than the 2011 EPA national emission inventory (NEI11v1) estimate of $0.29\,Tg\,N\,month^{-1}$ ($0.28\,Tg\,N\,month^{-1}$ from the updated NEI11v2 emission inventory), although both inventories have a similar spatial distribution (Fig. S1 in the Supplement). We also apply a diurnal variation to anthropogenic NO_x emissions following Mao et al. (2013b). Soil NO_x emissions in our model, $3.6\,Tg\,N\,yr^{-1}$ globally (Naik et al., 2013), are considerably lower than other model estimates, including $5.5\,Tg\,N\,yr^{-1}$ in Yienger and Levy (1995) and $9.0\,Tg\,N\,yr^{-1}$ in Hudman et al. (2012). As a result, anthropogenic NO_x emissions over the continental US are 0.84 Tg N for July–August 2004, and 0.50 Tg N in July–August 2013, with a 40 % reduction from 2004 to 2013 (Table 1). This relative change in anthropogenic NO_x emissions is consistent with EPA estimates (https://www.epa.gov/air-emissions-inventories/air-pollutant-emissions-trends-data) and satellite observations (Krotkov et al., 2016; Lu et al., 2015). Compared to the NEI11v1 inventory, RCP8.5 used in our model shows similar relative differences in the Southeast US and nationally.

Table 1. Monthly averaged NO_x emissions in July–August 2004 and 2013 over North America (25–50° N, 130–70° W) and over the Southeast US (25–40° N, 100–75° W) in brackets from AM3.

Source Type	2004 (Tg N)	2013 (Tg N)
Anthropogenic	0.42 (0.19)	0.25 (0.11)
Biomass burning	8.4×10^{-3} (2.8×10^{-3})	8.4×10^{-3} (2.8×10^{-3})
Soils	2.9×10^{-2} (9.5×10^{-3})	2.9×10^{-2} (9.5×10^{-3})
Aircraft	8.8×10^{-3} (2.9×10^{-3})	8.0×10^{-3} (2.8×10^{-3})
Lightning	0.02 (0.01)	0.02 (0.01)
Total	0.49 (0.22)	0.32 (0.14)

2.2 Gas-phase chemistry

We apply the same isoprene mechanism as described by Li et al. (2016). A full list of the reactions can be found in Table S1. This mechanism is based on Mao et al. (2013b), but has been significantly revised to incorporate recent laboratory updates on isoprene oxidation by OH, ozone, and NO_3 (Schwantes et al., 2015; Bates et al., 2014, 2016; Peeters et al., 2014; St. Clair et al., 2016; Praske et al., 2015; Müller et al., 2014; Lee et al., 2014; Crounse et al., 2011). One major feature is the suppression of the δ-isoprene hydroxy peroxy radical (δ-ISOPO$_2$) and subsequent reaction pathways in the model, as these channels are considered to be of minor importance under ambient conditions (Peeters et al., 2014; Bates et al., 2014). The fraction of ISOPO$_2$ undergoing isomerization is calculated using bulk isomerization estimates (Crounse et al., 2011). As a result, the first-generation isoprene alkyl nitrate is assumed to be β-hydroxy nitrate (ISOPNB) in the model with a yield of 10 % from the ISOPO$_2$ + NO pathway. This differs from a recent GEOS-Chem study of organic nitrates over the Southeast US that assumed a 9 % yield of the first-generation isoprene alkyl nitrate comprised of 90 % ISOPNB and 10 % δ-hydroxy nitrate (ISOPND; Fisher et al., 2016). The treatment of β- and δ-ISOPO$_2$ will not only affect the speciation of organic nitrates but also the production of ozone due to different NO_x recycling efficiency in their secondary products. We also include updated chemistry for methylvinyl ketone (MVK; Praske et al., 2015), an updated yield of hydroxy hydroperoxides (ISOPOOH; Bates et al., 2016; St. Clair et al., 2016), fast photolysis of carbonyl organic nitrates (Müller et al., 2014), and an updated ozonolysis rate of ISOPNB (Lee et al., 2014). In addition, we reduce the yield of organic nitrates (MACRN) from methacrolein (MACR) oxidation from 15 to 3 %, which is estimated from the measured yield of nitrates from MVK oxidation (Praske et al., 2015).

Another major model revision involves the treatment of the nighttime oxidation of isoprene. Instead of following Mao et al. (2013b), we revise the nighttime oxidation of isoprene largely based on the Leeds Master Chemical Mechanism v3.2 (MCM v3.2), allowing for a more complete description of isoprene oxidation by NO_3. In particular,

MCM v3.2 suggests significant production of propanone nitrate (PROPNN) from the photooxidation of the C$_5$ carbonyl nitrate, which is consistent with recent laboratory experiments (Schwantes et al., 2015). We also update the products of the reaction of the nitrooxy alkylperoxy radical (INO$_2$), the peroxy radical from isoprene oxidation by NO$_3$, with HO$_2$ to reflect a lower molar yield (0.77) of C$_5$ nitrooxy hydroperoxide (INPN; Schwantes et al., 2015). The differences between MCM v3.2 and the most updated version, MCM v3.3.1, in isoprene nighttime chemistry appears to be small (Jenkin et al., 2015). We therefore use MCM v3.2 as the reference in this work.

We include a highly simplified chemistry for the oxidation of monoterpenes in this work, mainly to quantify their contribution to organic nitrates. Monoterpenes are lumped into one chemical species (C$_{10}$H$_{16}$) in our model. The organic nitrate yield is set to 26 % from OH-initiated oxidation (Rindelaub et al., 2015) and to 10 % from NO$_3$-initiated oxidation (Browne et al., 2014). Details of the monoterpene chemistry can be found in Table S2 in the Supplement.

2.3 Heterogeneous loss of organic nitrates

Field and laboratory studies have indicated a potential contribution to the aerosol formation of organic nitrates from BVOC oxidation (Ayres et al., 2015; Fry et al., 2009, 2014; Nah et al., 2016; Rollins et al., 2009; Rindelaub et al., 2015; Boyd et al., 2015, 2017; Lee et al., 2016; Ng et al., 2008; Xu et al., 2015; Lee et al., 2014; Bean and Hildebrandt Ruiz, 2016; Spittler et al., 2006). Aerosol yield depends on both the VOC precursor and the oxidant. For example, Δ-3-carene oxidation by NO$_3$ can produce a 38–65 % yield of organic aerosols in a smog chamber (Fry et al., 2014), which is much higher than the 1–24 % yield from NO$_3$-initiated isoprene oxidation (Ng et al., 2008; Rollins et al., 2009; Ayres et al., 2015). Recent chamber studies indicate a very low aerosol yield from α-pinene oxidation by NO$_3$ (Nah et al., 2016; Fry et al., 2014); the aerosol yield increases to $\sim$ 18 % when α-pinene is oxidized by OH (Rollins et al., 2010; Rindelaub et al., 2015). However, these results might not be representative of atmospheric conditions in terms of the RO$_2$ reaction partner or RO$_2$ lifetime, warranting further studies on the effects

of RO_2 fates on aerosol formation (Boyd et al., 2015, 2017; Ng et al., 2008; Schwantes et al., 2015).

In the condensed phase, organic nitrates can undergo hydrolysis reactions producing HNO_3 (Darer et al., 2011; Hu et al., 2011; Rindelaub et al., 2015; Boyd et al., 2015; Szmigielski et al., 2010; Sato, 2008; Jacobs et al., 2014; Bean and Hildebrandt Ruiz, 2016). However, the hydrolysis rate varies greatly with structures of organic nitrates (Bean and Hildebrandt Ruiz, 2016; Darer et al., 2011; Hu et al., 2011; Boyd et al., 2015; Rindelaub et al., 2016). Here we assume a first-order irreversible reactive uptake for the heterogeneous loss of organic nitrates onto aerosols (Reaction R1), followed by their hydrolysis reaction returning HNO_3 and alcohols (Reaction R2; Fisher et al., 2016):

$$RONO_2(g) \xrightarrow{k_1} AONJ(aq), \tag{R1}$$

$$AONJ(aq) + H_2O \xrightarrow{k_2} ROH + HNO_3(g), \tag{R2}$$
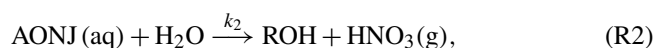
where $RONO_2$, AONJ, and ROH represent gas- and particle-phase organic nitrates and alcohols, respectively. We allow the heterogeneous loss of organic nitrates to sulfate, black carbon, primary organic carbon, sea salt, mineral dust, and SOA following Mao et al. (2013a). Besides the base case that only includes ISOPNB for heterogeneous loss (Jacobs et al., 2014), we include two additional sensitivity tests to evaluate the potential impact of organic nitrate hydrolysis. One is the "hydro_full" case including the heterogeneous loss of a C_5 dihydroxy dinitrate (DHDN) and monoterpene nitrates only from OH oxidation during daytime (TERPN1; nighttime monoterpene nitrates are excluded), and the other is the "no_hydro" case assuming no heterogeneous loss for any organic nitrate. We adopt an effective uptake coefficient of 0.005 for ISOPNB and DHDN and 0.01 for TERPN1, following Fisher et al. (2016), with a 3 h bulk lifetime in the particle phase (Pye et al., 2015; Lee et al., 2016; Table S3 in the Supplement). The details of each case are listed in Table 2.

2.4 Observational datasets

We use measurements from a series of field campaigns (2004 ICARTT, 2013 SENEX, and 2013 SEAC[4]RS) to evaluate model performance on ozone, NO_x, HNO_3, PAN, ΣANs, and NO_y over the Southeast US in summer.

The ICARTT aircraft campaign provided a detailed characterization of tropospheric chemistry over the eastern US in the summer of 2004 (1 July–15 August 2004). Two aircraft, the NASA DC-8 and the NOAA WP-3D, were deployed to collect measurements of ozone, RON, isoprene, and its oxidation products. Here we focus on data including ozone, NO_x, HCHO (tunable diode laser (TDL) absorption spectrometry), HNO_3 (mist chamber–ion chromatograph by the University of New Hampshire and chemical ionization mass spectrometry (CIMS) by the California Institute of Technology), PAN, and ΣANs (including gas and aerosol $RONO_2$)

collected on the NASA DC-8 aircraft over the Southeast US. Details of the instrument operation and accuracy are summarized in Singh et al. (2006) and the references therein.

Two aircraft campaigns were conducted in the summer of 2013 over the Southeast US. The first is the NOAA SENEX campaign using NOAA WP-3D aircraft to investigate the interaction between biogenic and anthropogenic emissions and the formation of secondary pollutants (27 May–10 July 2013). We focus on daytime measurements of ozone, NO_x, HNO_3, PAN, speciated $RONO_2$, and NO_y in this work. Details of the instrument operation and accuracy are summarized in Warneke et al. (2016) and the references therein. The second is the NASA SEAC[4]RS campaign, which took place in August–September 2013, with a focus on vertical transport of atmospheric pollutants from the surface to the stratosphere. Here we focus on observations of ozone, NO_2, HCHO (laser-induced fluorescence, or LIF), ΣANs (including gas and aerosol $RONO_2$), and speciated $RONO_2$ collected on the NASA DC-8 aircraft to evaluate model representation of ΣANs and $RONO_2$ originating from isoprene oxidation. Details of the instrument operation and accuracy are summarized in Toon et al. (2016) and the references therein.

Besides these aircraft campaigns, we also use surface observations for model evaluation, including nitrate (NO_3^-) wet deposition flux and concentration from the National Trends Network (NTN) of NADP (accessible at http://nadp.sws.uiuc.edu/data/) and surface ozone and NO_y from EPA AQS (accessible at https://aqs.epa.gov/aqsweb/documents/data_mart_welcome.html). We focus on NO_3^- wet deposition fluxes at 53 NADP sites and MDA8 ozone at 157 EPA AQS sites (Fig. S2 in the Supplement) in the Southeast US during July–August 2004 and 2013. NO_y measurements at 10 out of the 157 AQS sites in the same episodes are compared with model estimates as an additional constraint on the decadal changes in NO_y. We choose July–August as our "summer" since this is the common period of all the measurements used in the model evaluation.

3 Model evaluation

We evaluate our model against observations from aircraft campaigns in 2004 and 2013. For each of the three field campaigns, all measurements are averaged to a 1 min time resolution. Data from biomass burning ($CH_3CN \geq 225$ ppt or $HCN \geq 500$ ppt), urban plumes ($NO_2 \geq 4$ ppb or $NO_x / NO_y \geq 0.4$ if NO_y is available), and stratospheric air ($O_3 / CO > 1.25$ mol mol^{-1}) are excluded (Hudman et al., 2007) in all the analyses, as these subgrid processes may not be well represented in our model. We focus on the Southeast US region using data within the domain of 25–40° N latitude and 100–75° W longitude for our analyses. A map of all the flight tracks of each campaign is shown

in Fig. S3 in the Supplement. All model results are sampled along the flight track with 1 min time resolution.

3.1 Mean vertical profiles of ozone and RON

Figure 1 shows the observed and modeled mean vertical profiles of ozone, NO_x, HNO_3, PAN, ΣANs, and NO_y during ICARTT and SENEX. We use ΣANs measurements from SEAC^{4}RS to evaluate model performance during summer 2013 due to the lack of ΣANs measurements from SENEX. Our model results include both gas and aerosol $RONO_2$ in ΣANs, although aerosol $RONO_2$ accounts for 7–11 % of ΣANs in the planetary boundary layer (PBL, < 1.5 km). We do not consider inorganic nitrates in the particle phase in this analysis due to the lack of a thermodynamic model for inorganic aerosols in the current version of AM3. This simplification is expected to have minimal effects, as they only account for a small fraction of aerosol nitrates in the Southeast US (Ng et al., 2017). To investigate the impact of $RONO_2$ hydrolysis, we include two model simulations: the base case with heterogeneous loss of ISOPNB and a sensitivity run, "no_hydro", without heterogeneous loss of organic nitrates.

Mean observed ozone in the surface layer decreased from 50 ppb during ICARTT to 35 ppb during SENEX, which is consistent with the declining trend in surface MDA8 ozone at AQS monitoring sites (Sect. 4.2). As we show in Sect. 4.2, this decline in ozone is mainly driven by NO_x emission reduction, with little influence by meteorology in the two years. Our model can reproduce the vertical gradient and the relative change in ozone from 2004 to 2013, except for a positive absolute bias of 6–12 ppb in the boundary layer. The performance statistics of ozone in the boundary layer listed in Table S4 also indicate positive biases in the model, with a fractional bias (FB) of 9.4–17 %, fractional error (FE) of 16–19 %, normalized mean bias (NMB) of 9.4–16 %, and normalized mean error (NME) of 16–19 %. This overestimate of ozone is higher than that reported (3–5 ppb) by Mao et al. (2013b) for their simulation of the ICARTT dataset, likely due to faster photolysis of carbonyl nitrates that increases the NO_x recycling efficiency from isoprene oxidation.

We further examine mean vertical profiles of NO_x and its reservoirs in 2004 and 2013 (Fig. 1). In the boundary layer along the flight tracks, HNO_3 is the most abundant RON, accounting for 40–46 % of NO_y, followed by NO_x (18–23 %), PAN (20 %), and ΣANs (11–21 %). Between 2004 and 2013, mean observed NO_y in the boundary layer decreased by 20 %, from 2.0 to 1.6 ppb, a weaker change than the 35 % reduction of total NO_x emissions (Table 1). The responses of major RON species are mostly proportional to the change in NO_x emissions, with the notable exception of ΣANs. We find significant decreases in NO_x (−35 %) and HNO_3 (−29 %) as well as a slight decrease in PAN (−13 %) from observations. The relative trends of HNO_3 and PAN are opposite to those found in the Los Angeles (LA) basin, where PAN decreased much faster than HNO_3 (Pollack et

al., 2013). This difference results mainly from the rapid decrease in anthropogenic VOC emissions in the LA basin that also serve as major precursors of PAN. In contrast, isoprene is the major precursor of PAN over the Southeast US. Its emissions show a constant supply (within 5 % differences over the two summers) in this region. Showing a different trend from the above compounds, ΣANs increase from 0.23 to 0.27 ppb (+17 %) near the surface. As we show below in Sect. 4.1, these changes (except for ΣANs) are mostly consistent with model estimates on regional average. The discrepancy in their trends of vertical profiles and regional average might be due to representative errors from the three aircraft campaigns on spatial (Fig. S3 in the Supplement) and temporal (different episodes; refer to the observation data description in Sect. 2.4) scales.

The model can reproduce RON species in the boundary layer but tends to underestimate them in the free troposphere. This is likely due to insufficient production of NO_x from lightning in the free troposphere in our model, which is 0.048 Tg N in total over North America during July–August of 2004, lower by almost a factor of 5 compared to the value (0.27 Tg N from 1 July–15 August 2004) reported by Hudman et al. (2007). This underestimate can be improved by scaling up lightning emission by a factor of 5–10 (Fang et al., 2010). We do not adjust the lightning NO_x emission in this work due to its high uncertainty (Ott et al., 2010; Pickering et al., 1998).

The hydrolysis of organic nitrates affects $RONO_2$ significantly in the boundary layer. By introducing the hydrolysis of ISOPNB, we find that the model relative bias of ΣANs is reduced from +20 to +2 % during ICARTT (Fig. 1). The performance metrics in Table S4 in the Supplement also indicate better agreement of the model with observations if hydrolysis of ISOPNB assumed. However, the relative bias is increased in magnitude from −9 to −24 % during SEAC^{4}RS. This low bias can be partially due to neglecting small alkyl nitrates, which could contribute 20–30 ppt to ΣANs (less than 10 % near the surface) during SEAC^{4}RS (Fisher et al., 2016). Including small alkyl nitrates will increase modeled ΣANs a bit in ICARTT as well. The hydrolysis of ISOPNB also leads to a slight increase in HNO_3 (Table S4 in the Supplement). The impact of the hydrolysis of ISOPNB on boundary layer ozone appears to be small. This is mainly because without hydrolysis, the dominant loss of ISOPNB is oxidation by OH, which then leads to the formation of secondary organic nitrates including MVKN, MACRN, and DHDN. The majority of these organic nitrates (MVKN and DHDN) return NO_x slowly due to their long lifetimes (Table S5 in the Supplement), resulting in a similar effect on ozone production as the hydrolysis of ISOPNB. In addition to the good agreement of ΣANs, our model shows good agreement with speciated $RONO_2$ measured during SENEX and SEAC^{4}RS, including ISOPN and the sum of MVKN and MACRN (Fig. 2). We find that the large discrepancy between ΣANs and speciated alkyl nitrates (Fig. S4 in the Supplement) can be explained
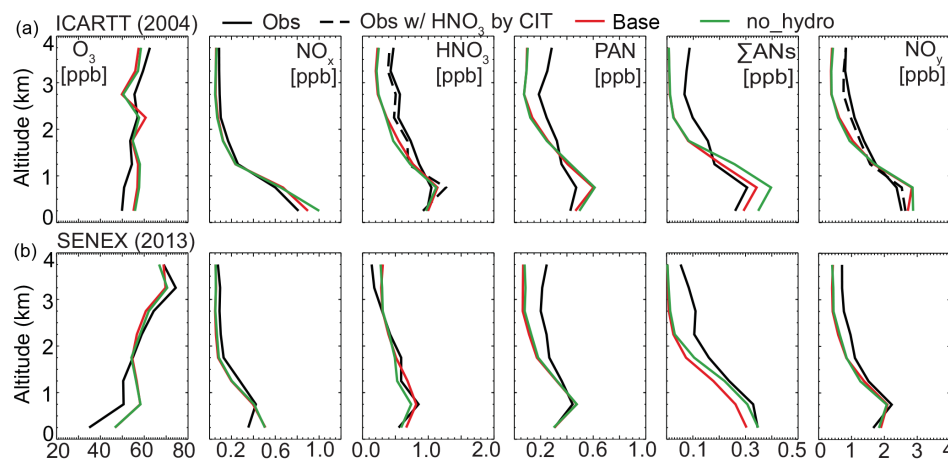
Figure 1. Mean vertical profiles of ozone and reactive oxidized nitrogen from observations during ICARTT **(a)** and SENEX **(b)** over the Southeast US (25–40° N, 100–75° W) during daytime and model estimates from AM3 with hydrolysis of ISOPNB (red) and AM3 without hydrolysis of alkyl nitrates (green). The solid and dashed black lines in the HNO₃ of ICARTT represent measurements collected using mist chamber–ion chromatograph by the University of New Hampshire (UNH) and chemical ionization mass spectrometry by the California Institute of Technology (CIT), respectively. NO_y from ICARTT is calculated as the sum of NO_x, HNO₃ (UNH in the solid line and CIT in the dashed line), PAN, and total alkyl nitrates (ΣANs). Observed and modeled ΣANs in **(b)** are during SEAC⁴RS.
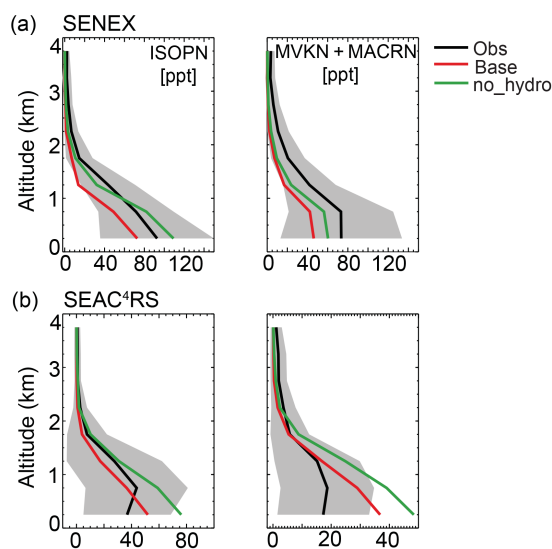
Figure 2. Mean vertical profiles of ISOPN and MVNK + MACRN during **(a)** SENEX and **(b)** SEAC⁴RS over the Southeast US (25–40° N, 100–75° W). Black lines are the mean of observations. Red and green lines are the mean of modeled results with hydrolysis of ISOPNB and without hydrolysis of alkyl nitrates, respectively. Gray shades are 1 standard deviation ($\pm\sigma$) of averaged profiles of the measured tracers.

by a combination of monoterpene nitrates and DHDN and nighttime NO_3 oxidation products from isoprene, accounting for 20–24, 14–17, and 23–29 % of ΣANs, respectively, in the boundary layer.

Given the good agreement between observed and modeled RON in both 2004 and 2013, we find that the ozone

bias shown in Fig. 1 cannot be completely explained by an overestimate of anthropogenic NO_x emissions. A recent GEOS-Chem study (Travis et al., 2016) shows that the ozone bias can be largely reduced by scaling down anthropogenic NO_x emissions. We find that a similar reduction of anthropogenic NO_x emissions in 2013, from 0.25 Tg N month⁻¹ to 0.15 Tg N month⁻¹, would lead to an underestimate of NO_y, HNO₃, and PAN by 30, 33, and 30 %, respectively. Such a reduction would also be inconsistent with the relative changes in EPA estimates of NO_x emissions shown above. Indeed, other processes, such as ozone dry deposition, may also contribute to this bias and warrant further investigation.

3.2 NO_3^- wet deposition flux and concentration

Figure 3 shows a comparison of NO_3^- wet deposition flux between observations and model results during the summers of 2004 and 2013. The observed NO_3^- wet deposition flux is calculated by multiplying the measured NO_3^- concentration and precipitation at each monitoring site as $F_{o,i} = C_{o,i} P_{o,i}$, where $F_{o,i}$ is the monthly mean NO_3^- wet deposition flux, $C_{o,i}$ and $P_{o,i}$ are the monthly mean observed NO_3^- concentration and precipitation at monitoring site i. The modeled NO_3^- wet deposition flux includes HNO₃ and all the alkyl nitrates. Observations indicate a 24 % reduction of NO_3^- wet deposition flux in summer from 2004 to 2013 over the Southeast US, likely due to NO_x emission reductions. This reduction in monthly averaged NO_3^- wet deposition flux is well captured by our model (−29 %), despite a low relative bias of 40 % in both years and NMB of −39 to −43 % (Table S4 in the Supplement).
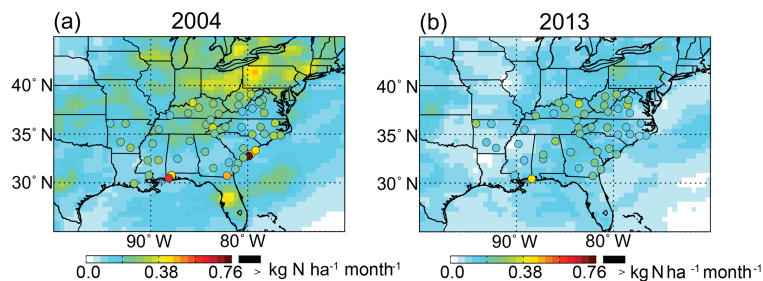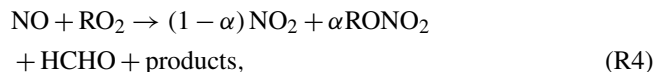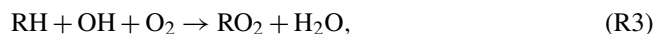
Figure 3. Nitrate wet deposition flux ($kg\,N\,ha^{-1}\,month^{-1}$) from NADP (circles) and AM3 (background) during July–August of 2004 and 2013.

Since errors in modeled precipitation could strongly affect the modeled NO_3^- wet deposition flux (Appel et al., 2011; Grimm and Lynch, 2005; Metcalfe et al., 2005; Paulot et al., 2014; Tost et al., 2007), we also evaluate the modeled NO_3^- concentration ($C_{p,i}$), which is calculated by using the modeled NO_3^- wet deposition flux ($F_{p,i}$) and observed precipitation ($P_{o,i}$; $C_{p,i} = F_{p,i}/P_{o,i}$), as a separate constraint. The model shows a similar declining trend from the observations with a relative bias of -23 and -41% in NO_3^- concentration for 2004 and 2013, respectively. Our results are consistent with the base case of Paulot et al. (2016), which showed that convective removal is likely insufficient in AM3, leading to underestimates of both NO_3^- wet deposition flux and concentrations. Our results are somewhat different from a recent GEOS-Chem study (Travis et al., 2016). The authors found that reducing anthropogenic NO_x emissions from NEI11v1 by 53 % can significantly improve the overestimate of 71 % for NO_3^- wet deposition flux in their model during August–September of 2013. A further reduction of anthropogenic NO_x emissions in our model (to $0.15\,Tg\,N\,month^{-1}$), as suggested by Travis et al. (2016), would lead to an even greater negative bias compared to observations.

3.3   RONO₂ and related species

We further evaluate $RONO_2$ and related species in this section, with a large focus on measurements from ICARTT and SEAC⁴RS. The major pathway for the production of daytime $RONO_2$ is the reaction of NO with RO_2 originating from VOC oxidation by OH:

$$RH + OH + O_2 \rightarrow RO_2 + H_2O, \tag{R3}$$

$$NO + RO_2 \rightarrow (1 - \alpha)\,NO_2 + \alpha RONO_2$$
$$+ HCHO + products, \tag{R4}$$

where α is the branching ratio for alkyl nitrate formation. NO_2 subsequently undergoes photolysis to produce ozone:

$$NO_2 + h\nu \xrightarrow{O_2} O_3 + NO. \tag{R5}$$

For isoprene, α is $9 \pm 4\%$ (for ISOPN) according to a recent study (Xiong et al., 2015). For monoterpenes, specifically α-pinene, α ranges from 1 to 26 % (Rindelaub et al., 2015;

Nozière et al., 1999; Aschmann et al., 2002). Here, we use 10 % for isoprene and 26 % for monoterpenes. As $RONO_2$ and ozone are both produced from Reaction R4, a correlation between them is expected. We show that the model can roughly reproduce the correlation of O_x ($= O_3 + NO_2$) vs. ΣANs during both ICARTT and SEAC⁴RS (Fig. 4), although the slope has a positive relative bias of about 21 and 33 %, respectively, largely due to an overestimate of ozone in the model. The good agreement between observed and modeled O_x vs. daytime $RONO_2$ provides additional support for our treatment of the yields and fate of these daytime isoprene nitrates.

Another metric to evaluate $RONO_2$ chemistry is the correlation between ΣANs and HCHO, as the latter is a co-product from Reaction R4. We show in Fig. 4 that the model can roughly capture the observed ΣANs–HCHO slope, with an underestimate by 25 and 13 % during ICARTT and SEAC⁴RS, respectively. The underestimate is in part due to small alkyl nitrates that are neglected in the model, as mentioned in Sect. 3.1. During ICARTT, the slope estimated by AM3 is 0.12, similar to the value (0.15) from a previous GEOS-Chem study using a different isoprene oxidation mechanism that assumed a higher α (of 4.7 % from ISOPNB and 7.0 % from ISOPND vs. 10 % of ISOPNB and zero ISOPND in AM3) and a lower yield of HCHO (66 % vs. 90 % in AM3; Mao et al., 2013b). The reason for such similarity between the two models might be twofold: (a) the additional contribution of monoterpene nitrates to ΣANs in AM3 compensates for the decrease in α from isoprene nitrates compared to GEOS-Chem and (b) the coarse grid resolution of GEOS-Chem simulations ($2° \times 2.5°$) may lead to a higher estimate of HCHO compared to the result from a finer grid resolution (Yu et al., 2016).

Since HCHO can be produced from pathways of isoprene hydroxy peroxy radicals ($ISOPO_2$) other than Reaction R4 (such as isomerization of $ISOPO_2$ and $ISOPO_2 + HO_2$), changes in the slope of ΣANs vs. HCHO may help to quantify decadal changes in isoprene oxidation pathways. We find in Fig. 4 that the observed slope of ΣANs-HCHO shows very little change from 2004 to 2013. This is in part due to substantial HCHO production from isoprene oxidation un-
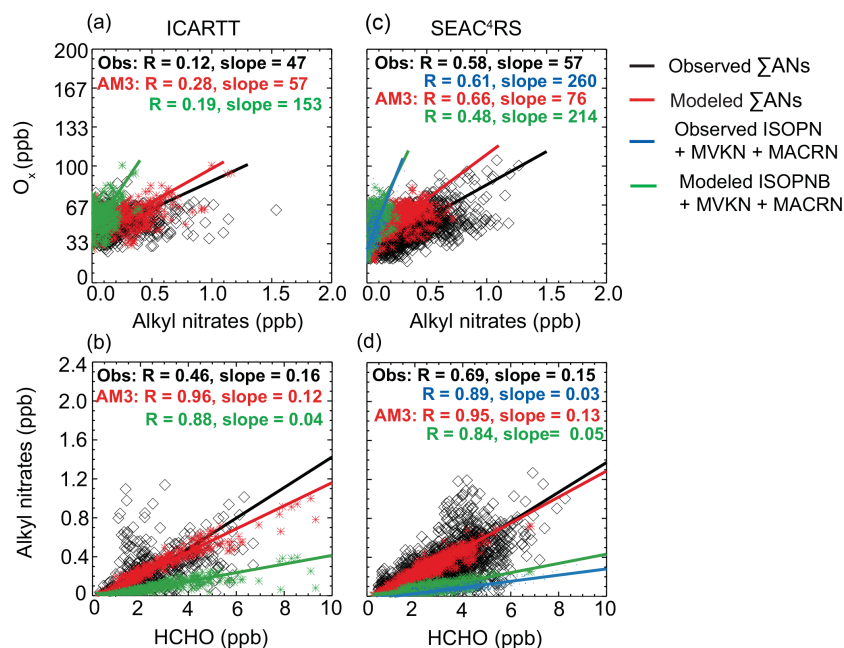
Figure 4. O_x versus ΣANs correlation **(a, c)** and ΣANs versus formaldehyde correlation **(b, d)** within the boundary layer (< 1.5 km) during ICARTT **(a, b)** and SEAC[4]RS **(c, d)**. Observations are in black diamonds; model estimates from AM3 with ISOPNB hydrolysis are represented by red symbols. Green symbols represent the correlation using modeled ISOPN + MVKN + MACRN. Blue symbols represent the correlation using observed ISOPN + MVKN + MACRN from SEAC[4]RS. Solid lines are the reduced major axis regression lines.
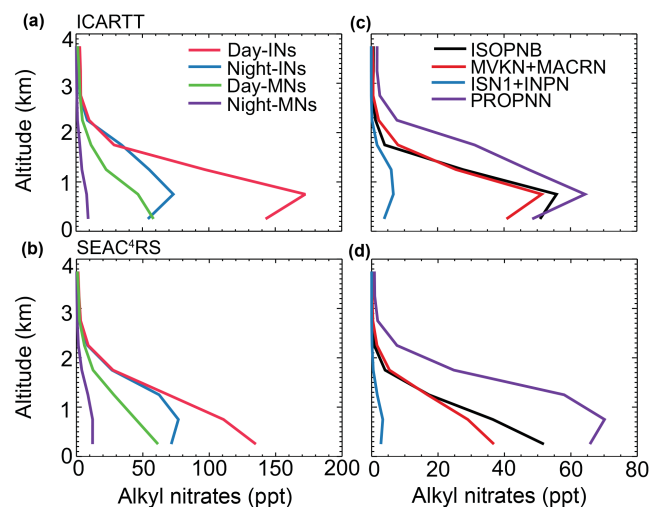
Figure 5. Mean vertical profiles of modeled alkyl nitrates from isoprene and monoterpene oxidation **(a, b)** and major isoprene nitrate species **(c, d)** during ICARTT **(a, c)** and SEAC[4]RS **(b, d)** from AM3 with hydrolysis of ISOPNB.

der low NO_x conditions (Li et al., 2016) and in part due to the buffering of ΣANs in response to decreasing NO_x, as shown below in Sect. 4.1. Our model is able to reproduce such behavior. We also find that the branching ratios for the reactions of $ISOPO_2$ change marginally from 2004 to 2013 over the Southeast US (Fig. S5 in the Supplement). The frac-

tion of $ISOPO_2 + NO$ decreases from 81 % in 2004 to 66 % in 2013. The fraction of $ISOPO_2 + HO_2$ increases from 15 to 28 %, and the fraction of $ISOPO_2$ isomerization increases from 4 to 6 %. Our results are slightly different from the results of GEOS-Chem, which found a lower contribution from the NO pathway (54 %) and a higher contribution from isomerization (15 %) during August–September of 2013 (Travis et al., 2016).

We also compare the correlation between major daytime isoprene nitrates and HCHO during 2013, which provides a constraint on the yield of these nitrates. Our model shows a slight overestimate on the slope (Fig. 4d), which is consistent with the comparison of mean vertical profiles shown in Fig. 2. The computed slope (5 %) in this study is different from that (2.5 %) of a recent GEOS-Chem simulation by Fisher et al. (2016). This is partially due to the different treatment of β- and δ-$ISOPO_2$ between GEOS-Chem and AM3. Another factor is that MVKN and MACRN are not allowed to hydrolyze in AM3, leading to a higher abundance of these two nitrates.

Figure 5 shows the mean vertical profiles of modeled monoterpene nitrates (MNs) and isoprene nitrates (INs) during ICARTT and SEAC[4]RS. INs are the most abundant $RONO_2$, accounting for 76–80 % below 3 km over the Southeast US. In the measurements, ISOPN + MVKN + MACRN only contributes one-third of ΣANs (Fig. S4 in the Supplement). We show below that the discrepancy between ΣANs and speciated $RONO_2$ can be explained by other daytime and

nighttime INs and MNs in the model. More than 60 % of modeled INs originate from isoprene oxidation during daytime. The first-generation nitrate ISOPN contributes slightly more (31 %) than the second-generation nitrates MVKN + MACRN (28 %) to the total daytime INs during ICARTT. This is different from Mao et al. (2013b), who showed a higher contribution of MVKN + MACRN than the first-generation INs due to the different treatment of β- and δ-ISOPO$_2$. We see more ISOPN (32 %) than MVKN + MACRN (26 %) from the daytime INs during SEAC^{4}RS, which is consistent with Fisher et al. (2016). A large uncertainty in our model is attributed to DHDN, which contributes 32 % to the daytime INs. Fisher et al. (2016) showed less DHDN during SEAC^{4}RS since it was removed rapidly by hydrolysis (1 h lifetime) in their model. Our sensitivity test (hydro_full; Fig. S6 in the Supplement) indicates that AM3 would significantly underestimate ΣANs if we assume a similar heterogeneous loss of DHDN as ISOPN. In fact, DHDN was hypothesized originally in Lee et al. (2014) for the imbalance of nitrogen in their lab experiments, and may serve as a proxy for a large number of unidentified daytime INs. It remains unclear what the dominant loss of DHDN is. Daytime nitrates from monoterpene oxidation are another important source of ΣANs in this region, accounting for 17–20 % (24–26 ppt) of the total. Fisher et al. (2016) estimate a smaller burden of MNs of about 10–20 ppt due to a lower molar yield (18 % vs. 26 % in AM3) and faster hydrolysis of MNs in their model.

Nighttime chemistry contributes about 30–36 % of ΣANs, which is dominated by isoprene oxidation as well (Fig. 5). About 33–41 % of the INs are produced during night, similar to the value (44 %) reported by Mao et al. (2013b) but with different speciation due to the different treatment of chemistry. PROPNN contributes about 29–38 % of the total INs. PROPNN in this work is mainly produced from the oxidation of C$_5$ nitrooxy hydroperoxide (INPN) and C$_5$ carbonyl nitrate (ISN1; dominantly by photolysis) that are generated from isoprene oxidation by NO$_3$ during the nighttime. This is different from Fisher et al. (2016), who showed that PROPNN is partially from the δ-ISOPO$_2$ + NO pathway and partially from the oxidation of ISN1 by NO$_3$. In our model, we see a rapid increase in PROPNN after sunrise in the boundary layer (Fig. S7 in the Supplement), which is consistent with observations at the Southern Oxidants and Aerosols Study (SOAS) ground site CTL (Schwantes et al., 2015). Our model overestimates the mean vertical profile of PROPNN by a factor of 3 (not shown). As our model may largely underrepresent the chemical complexity of nighttime isoprene oxidation as shown by Schwantes et al. (2015), we consider PROPNN as a proxy for other unspecified isoprene nighttime nitrates. Overall, PROPNN contributes a significant fraction of ΣANs in the model, 23–29 % in the boundary layer as shown in Sect. 3.1. With monoterpene nitrates and isoprene-derived DHDN and nighttime NO$_3$ oxidation products taken into account, we find that our model can reproduce both ob-

served ΣANs and speciated alkyl nitrates (Fig. S4 in the Supplement).

4 Decadal changes in PBL RON and surface ozone over the Southeast US

As RON and related species from aircraft and surface measurements are well reproduced in our model in the summers of 2004 and 2013, we assume that the model is representative of this chemical environment and then use the model to derive monthly mean changes between the summers of 2004 and 2013. We also investigate the impacts of further decreases in NO$_x$ emissions by applying a hypothetical 40 % reduction of anthropogenic NO$_x$ emissions in 2013 but keeping other emissions and meteorology the same (the "hypo" case in Table 2).

4.1 PBL RON

We first examine the simulated decadal changes in RON in the boundary layer over the Southeast US as shown in Fig. 6. In the summer of 2004, the model suggests that NO$_y$ is mainly comprised of HNO$_3$ (45 %), NO$_x$ (31 %), ΣPNs (14 %), and ΣANs (9 %). In response to a 40 % reduction in anthropogenic NO$_x$ emissions (35 % reduction in total NO$_x$ emissions; Table 1) from 2004 to 2013, NO$_y$ declines by 34 %. This modeled response is comparable to long-term NO$_y$ measurements from the AQS surface network, which shows on average a 45 % decrease from 2004 to 2013 over the Southeast US. Based on model estimates in Fig. 6, most RON species are reduced proportionally, with decreases of 38 % for HNO$_3$, 32 % for NO$_x$, and 34 % for ΣPNs. The different changes in ΣPNs and PAN (the majority of ΣPNs) in Fig. 1 might be due to the difference in sampling regions. The only exception is ΣANs, with a smaller decline of 19 %. As an important source of organic aerosols, ΣANs may contribute to the decrease in organic aerosols over the Southeast US in the past decade (Blanchard et al., 2016).

We then conduct a sensitivity test with an additional 40 % reduction of anthropogenic NO$_x$ emissions from 2013. We find that NO$_y$ decreases by 29 %, with a proportional decrease in HNO$_3$, NO$_x$, and ΣPNs (Fig. 6). The slower decrease in NO$_y$ is likely due to ΣANs, which decrease at a slower rate and become a larger fraction of NO$_y$. The buffering of ΣANs is consistent with previous studies (Browne and Cohen, 2012; Fisher et al., 2016), mainly due to lower OH resulting from decreased NO$_x$ (Fig. S8) and thus prolonged lifetimes of NO$_x$ and ΣANs (Browne and Cohen, 2012). As shown in Fig. S8 in the Supplement, averaged noontime OH decreases by 11 % from 2004 to 2013 and by 29 % after we impose an additional 40 % reduction of anthropogenic NO$_x$ emissions from 2013 levels.

The historical NO$_x$ emission reduction also affects reactive nitrogen export out of the boundary layer. Here we de-

Table 2. Case descriptions.

Case name	Heterogeneous loss of organic nitrates	NO_x emissions	Meteorology
base	ISOPNB with a γ of 0.005 and followed by a hydrolysis rate of $9.26 \times 10^{-5}\,s^{-1}$	2004 and 2013	2004 and 2013
no_hydro	–	2004 and 2013	2004 and 2013
hydro_full	ISOPNB and DHDN with a γ of 0.005 and followed by a hydrolysis rate of $9.26 \times 10^{-5}\,s^{-1}$; TERPN1 with a γ of 0.01 and followed by a hydrolysis rate of $9.26 \times 10^{-5}\,s^{-1}$	2004 and 2013	2004 and 2013
hypo	Same with the base case	40 % reduction of anthropogenic NO_x emissions of 2013	2013
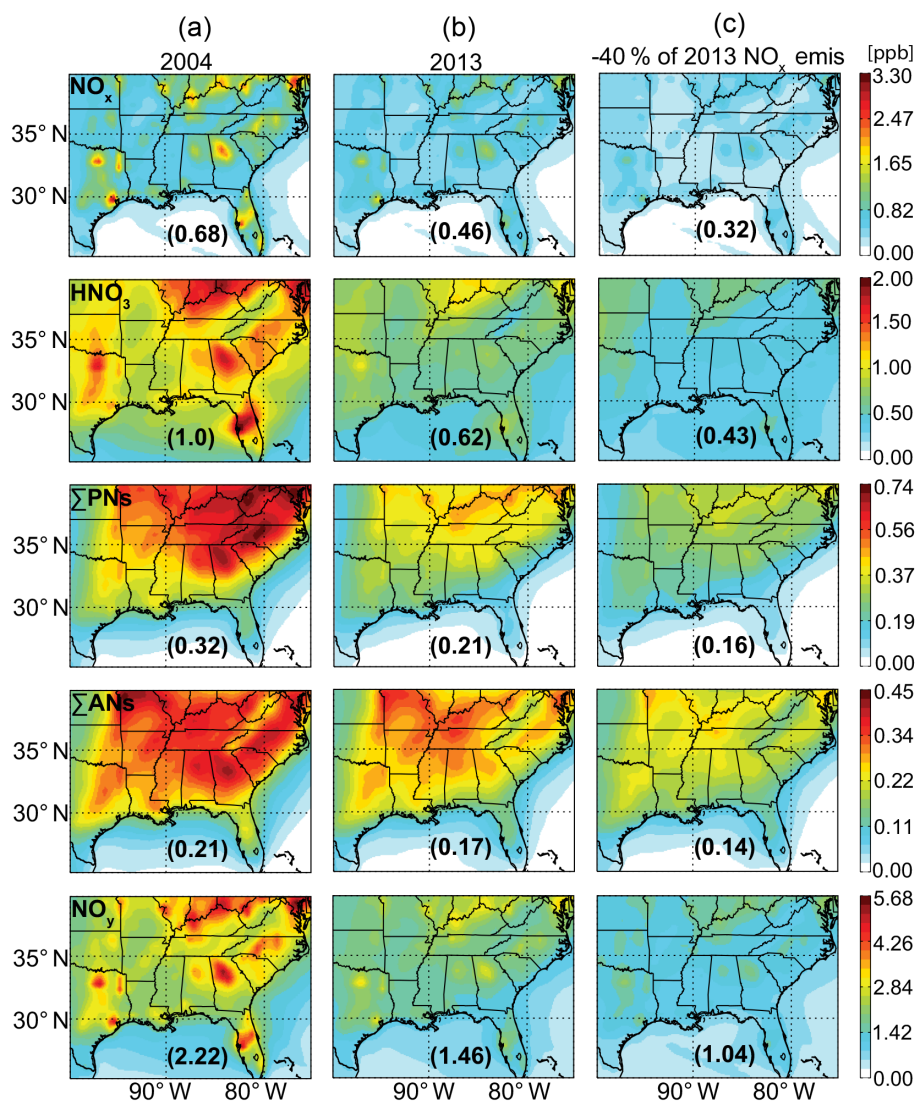
Figure 6. Modeled mean NO_x, HNO_3, total peroxy nitrates (ΣPNs), total alkyl nitrates (ΣANs), and NO_y averaged over the boundary layer (< 1.5 kmg) of the Southeast US during July–August of 2004 **(a)**, 2013 **(b)**, and a scenario assuming 40 % reduction of 2013 anthropogenic NO_x emissions **(c)**. Numbers in parentheses indicate mean concentrations over the plotted region. Note that different color scales represent the concentration of each species.

fine exported nitrogen as the difference of the sources (chemical production and emissions) and sinks (chemical loss, wet and dry deposition). As shown in Table 3, total summertime NO_y export from the Southeast US boundary layer decreases proportionally, from 24.1 Gg N in 2004 to 16.6 Gg N in 2013. The NO_y export efficiency, calculated as net exported nitrogen divided by total NO_x emissions, remains roughly the same (12 %) for 2004 and 2013, which is comparable to previous studies (Fang et al., 2010; Li et al., 2004; Parrish et al., 2004; Mao et al., 2013b; Sanderson et al., 2008; Hudman et al., 2007). Among all exported species, NO_x contributes most to the net export from the PBL (6 % of total NO_x emissions), followed by PAN (4 %) and ΣANs (2 %). We emphasize in Table 3 that a major fraction of NO_x is exported through the top of the boundary layer (convection). From a budget calculation throughout the tropospheric column over the same region, we find that despite having the same NO_y export efficiency (12 %), HNO_3 becomes the major exporter, accounting for half of NO_y export efficiency from the total column (6 %). The contributions from PAN and ΣANs are roughly the same as their export from the boundary layer (4 and 2 %). This suggests that surface NO_x ventilated through the boundary layer, converted to HNO_3 in the free troposphere, and exported as HNO_3 is likely the major NO_y export mechanism over the Southeast US in our model, which is in agreement with previous observations (Parrish et al., 2004; Neuman et al., 2006). PAN and ΣANs together account for another half of NO_y export efficiency. As PAN and ΣANs are of biogenic origin and longer lived than HNO_3, they may play a key role in influencing RON and ozone in downwind regions (Moxim et al., 1996; Fischer et al., 2014).

4.2 Surface ozone

Since the mid-1990s, NO_x emission controls have led to significant improvement in ozone air quality over the eastern US (Simon et al., 2015; Cooper et al., 2012). As NO_x emissions continue to decrease, ozone production efficiency (OPE) may increase due to the lower NO_x removal rate by OH and to some extent may compensate for the ozone reduction (Sillman, 2000). Meanwhile, surface ozone production may be further complicated by the increasing importance of RO_2 isomerization and $RO_2 + HO_2$. Here we first evaluate our model against surface ozone observations in 2004 and 2013 and then project the future response of surface ozone to even lower NO_x emissions to examine the efficacy of near-term NO_x emission controls at lowering near-surface ozone levels.

We first examine the modeled surface ozone against observations at 157 EPA AQS monitoring sites over the Southeast US in July–August of 2004 and 2013 (Fig. S9 in the Supplement). In general, AM3 overestimates surface MDA8 ozone in both years by about 16 ppb on average, with NMB of 33–45 % and NME of 35–46 %. This positive bias of sum-

mertime surface ozone has been a common issue in a number of modeling studies of this region (Fiore et al., 2009; Canty et al., 2015; Brown-Steiner et al., 2015; Strode et al., 2015; Travis et al., 2016). This might be partially attributed to overestimated anthropogenic NO_x emissions from non-power plant sectors, excessive vertical mixing in the boundary layer (Travis et al., 2016), or underestimates of ozone dry deposition (Hardacre et al., 2015; Val Martin et al., 2014). Further studies are warranted to investigate the cause of this bias in AM3.

Surface ozone concentrations over the Southeast US decline substantially from 2004 to 2013 in response to the large NO_x emission reduction (Simon et al., 2015). MDA8 ozone averaged across all the monitoring sites is observed to decrease by 11 ppb (23 % of observed mean MDA8 ozone in July–August of 2004) resulting from an approximate 40 % reduction of anthropogenic NO_x emissions (35 % reduction in total NO_x emissions). This strong sensitivity of surface ozone to NO_x emissions reflects the linear relationship between the ozone production rate and NO_x concentrations when NO_x is low (Trainer et al., 2000). Our model is able to capture this strong NO_x–O_3 sensitivity, with the mean MDA8 ozone reduced by 10 ppb from 2004 to 2013. We find that a further 40 % reduction of anthropogenic NO_x emissions with identical meteorological conditions could lead to an additional 9 ppb decrease in MDA8 ozone, a similar magnitude to the change from 2004 to 2013.

We further investigate the impact of temperature and moisture on surface ozone from 2004 to 2013. While several studies suggest that surface ozone increases with ambient temperature (Jacob and Winner, 2009; Bloomer et al., 2010; Wu et al., 2008; Steiner et al., 2010), Cooper et al. (2012) showed that this temperature-related impact is weak during the period 1990–2010 across the USA. Recent studies suggest that relative humidity (RH) or vapor pressure deficit (VPD) may play an important role in ozone variability through soil–atmosphere or biosphere–atmosphere coupling (Kavassalis and Murphy, 2017; Camalier et al., 2007; Tawfik and Steiner, 2013). Our model shows marginal differences in RH (less than 1 %) and temperature (+2.4 K) within the PBL over the Southeast US between the summers of 2004 and 2013, which is consistent with observed changes in RH (+2.7 %) and temperature (+2.6 K) during ICARTT and SENEX. This small variation in the model is also consistent with climatology data (Hidy et al., 2014). Camalier et al. (2007) showed that RH has a much bigger impact on summertime ozone than temperature over the Southeast US, suggesting little influence of meteorology on ozone trends during this period. Using the same model but with the standard AM3 chemical mechanism, Lin et al. (2017) found that meteorology changes would have caused high surface ozone over the eastern US to increase by 0.2–0.4 ppb yr^{-1} in the absence of emission controls from 1988 to 2014. Therefore, we conclude that the impact of climate variability and change on surface ozone is relatively small compared to NO_x emission reductions over

Table 3. Monthly NO_y budget in the boundary layer (< 1.5 km) of the Southeast US during July–August of 2004, 2013, and a scenario with 40 % reduction of anthropogenic NO_x emissions of 2013[a].

Species	2004					2013					−40 % of 2013 anthropogenic NO_x emis				
	Emission	Chem (P-L)	Dry dep	Wet dep	Net export	Emission	Chem (P-L)	Dry dep	Wet dep	Net export	Emission	Chem (P-L)	Dry dep	Wet dep	Net export
NO_x	208.7	−172.4	21.8	–	14.5	132.6	−105	14.2	–	13.4	88.3	−69.6	9.2	–	9.5
ΣPNs[b]		15.2	5.7	–	9.5		10.3	3.9	–	6.4		7.7	3.0	–	4.7
ΣANs		24.3	14.3	6.2	3.8		19.4	11.4	4.7	3.3		15.4	9.1	3.9	2.4
Day[c]		13.8	8.7	3.6	1.5		12.0	7.5	3.0	1.6		10.2	6.3	2.6	1.3
Night[d]		10.5	5.6	2.6	2.4		7.4	4.0	1.7	1.7		5.3	2.8	1.3	1.1
HNO_3		131.7	77.8	57.6	−3.7		74.2	45.6	35.1	−6.5		45.8	29.2	25.6	−9.0
NO_y					24.1					16.6					7.6

[a] We define the boundary of the Southeast US as 25–40° N, 100–75° W. All budget terms are in Gg N.
[b] ΣPNs includes PAN, peroxymethacryloyl nitrate (MPAN), and a C_5 hydroxy peroxyacyl nitrate (C5PAN1) produced by oxidation of ISN1.
[c] Alkyl nitrates produced from oxidation of isoprene and monoterpenes by OH.
[d] Alkyl nitrates produced from oxidation of isoprene and monoterpenes by NO_3.
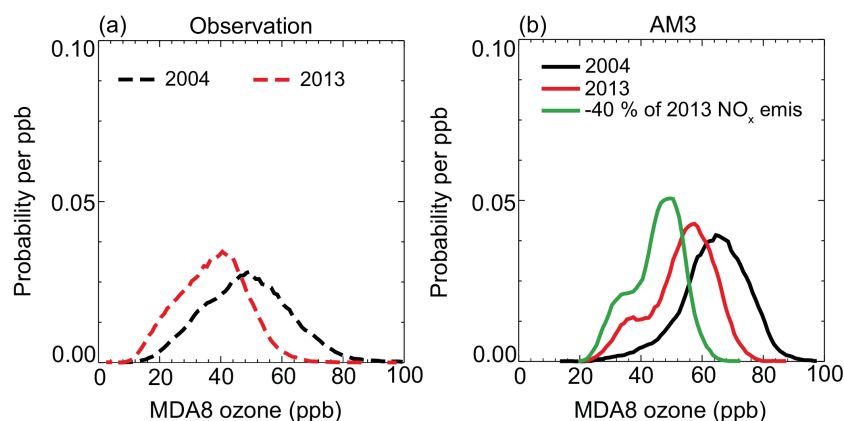
Figure 7. Observed (a) and simulated (b) probability density function of MDA8 ozone at AQS monitoring sites in Fig. S2 in the Supplement during the summers of 2004 and 2013 and a scenario with a 40 % reduction in the anthropogenic NO_x emissions of 2013.

the Southeast US, which is consistent with previous studies (Lam et al., 2011; Hidy et al., 2014; Lin et al., 2017; Rieder et al., 2015).

Decreasing NO_x emissions also reduce the frequency of high-ozone pollution events. Figure 7 shows the probability density function of observed and modeled MDA8 ozone at each monitoring site during July–August 2004 and 2013 and the probability density function of modeled MDA8 ozone under a hypothetical scenario with a 40 % reduction in anthropogenic NO_x emissions compared to 2013. We show that the lowest ozone, about 20 ppb in current model simulations, remains invariant with NO_x emission changes over the Southeast US, which is consistent with observations (Fig. 7a). Meanwhile, the high tail of MDA8 ozone events shifted from more than 100 ppb in 2004 to about 85 ppb after the 40 % reduction of anthropogenic NO_x emissions from 2013. A similar shift is found in observations. The narrowing of the range of ozone with decreasing NO_x is consistent with the observed trends reported by Simon et al. (2015). We also find that further reductions of NO_x emissions will reduce both median ozone values and the high tail, suggesting that fewer high-

ozone events will occur under continued NO_x emission controls in the future.

5 Conclusion and discussion

Near-surface ozone production over the Southeast US is heavily influenced by both anthropogenic and biogenic emissions. We investigate the response of NO_y speciation to the significant NO_x emission controls (about 40 % reduction) in this region over the past decade in light of the fast-evolving understanding of isoprene photooxidation. This knowledge is needed to predict nitrogen and ozone budgets in this region and elsewhere in the world with similar photochemical environments. Here we use extensive aircraft and ground observations combined with a global chemistry–climate model (GFDL AM3) to examine decadal changes in NO_y abundance and speciation as well as in surface ozone mixing ratios over the Southeast US between the summers of 2004 and 2013. We then use the model to infer future NO_y speciation and surface ozone abundances in response to further NO_x emission controls in this region.

We first evaluate the model with aircraft and surface observations. When we apply the estimated 40 % reduction in anthropogenic NO_x emissions from 2004 to 2013, our model reproduces the major features of the vertical profiles of NO_x, HNO_3, PAN, ΣANs, and NO_y observed during aircraft campaigns over the Southeast US in the summers of 2004 and 2013. By including recent updates to isoprene oxidation, our model can largely reproduce the vertical profiles of ΣANs and several speciated alkyl nitrates, as well as their correlations with O_x and HCHO, lending support to the model representation of isoprene oxidation. On the other hand, we show that a discrepancy between measured ΣANs and speciated $RONO_2$ can be explained by a combination of monoterpene nitrates, dinitrates, and nighttime NO_3 oxidation products from isoprene. We also show that modeled ozone appears to be insensitive to the hydrolysis of ISOPNB because its photooxidation, mainly by OH, also returns little NO_x.

Major RON species decline proportionally as a result of NO_x emission reductions in the Southeast US, except for a slower rate in ΣANs. The slower decline of ΣANs reflects the prolonged lifetime of NO_x when it is decreasing. Our model suggests that summertime monthly averaged NO_x, HNO_3, PAN, and NO_y decline by 30–40 % in response to a 40 % reduction in anthropogenic NO_x emissions from 2004 to 2013. This proportional decrease is likely driven by high concentrations of biogenic VOCs, the major precursor of PAN in this region that change little in magnitude from 2004 to 2013. In contrast, Pollack et al. (2013) find a faster PAN decrease than HNO_3 in the LA basin over the past several decades, partly due to the decrease in anthropogenic VOC emissions that are major PAN precursors.

Deposited and exported NO_y decline with NO_x emission reductions. The model also shows a decrease in NO_3^- wet deposition flux by 29 % from 2004 to 2013, which is consistent with observations from the NADP network (-24 %). We find from model calculations that the NO_y export efficiency remains at 12 % in both 2004 and 2013, leading to a proportional decrease in exported NO_y. The dominant NO_y export terms include NO_x and HNO_3, each accounting for 6 % of the total exported NO_y, followed by ΣPNs (4 %) and ΣANs (2 %).

The response of surface ozone to NO_x emission reductions reveals a strong NO_x–O_3 sensitivity in summertime over the Southeast US. Observations from the EPA AQS surface network suggest that mean MDA8 ozone during July–August decreased by 23 %, from 48 ppb in 2004 to 37 ppb, in 2013. Despite a positive absolute bias of up to 12 ppb in boundary layer ozone and 16 ppb in surface MDA8 ozone, our model shows a 10 ppb decrease in surface MDA8 ozone from 2004 to 2013, which is very close to the observed 11 ppb decrease from the EPA data. The bias of ozone in our model is not entirely attributed to uncertainties in NO_x emissions, as the overestimate suggested by earlier work would lead to an underestimate of NO_y (Travis et al., 2016). Care should be exercised in applying the modeling results for surface ozone regulation purposes given the high-ozone bias shown in our model. We find from model calculations that modeled MDA8 ozone will continue to decrease by another 9 ppb, assuming that anthropogenic NO_x emissions are reduced by 40 % from 2013 levels with meteorology and other emissions kept the same. In addition, further NO_x emission reduction leads to less frequent high-ozone events. This continued strong sensitivity of surface ozone to NO_x emissions can guide the development of effective emission control strategies for improving future air quality.

The Supplement related to this article is available online at https://doi.org/10.5194/acp-18-2341-2018-supplement.

Edited by: Nga Lee Ng
Reviewed by: three anonymous referees

References

Anderson, D. C., Loughner, C. P., Diskin, G., Weinheimer, A., Canty, T. P., Salawitch, R. J., Worden, H. M., Fried, A., Mikoviny, T., Wisthaler, A., and Dickerson, R. R.: Measured and modeled CO and NOy in DISCOVER-AQ: An evaluation of emissions and chemistry over the eastern US, Atmos. Environ., 96, 78–87, 2014.

Appel, K. W., Foley, K. M., Bash, J. O., Pinder, R. W., Dennis, R. L., Allen, D. J., and Pickering, K.: A multi-resolution assessment of the Community Multiscale Air Quality (CMAQ) model v4.7

wet deposition estimates for 2002–2006, Geosci. Model Dev., 4, 357–371, https://doi.org/10.5194/gmd-4-357-2011, 2011.

Aschmann, S. M., Atkinson, R., and Arey, J.: Products of reaction of OH radicals with α-pinene, J. Geophys. Res., 107, https://doi.org/10.1029/2001JD001098, 2002.

Astitha, M., Luo, H., Rao, S. T., Hogrefe, C., Mathur, R., and Kumar, N.: Dynamic evaluation of two decades of WRF-CMAQ ozone simulations over the contiguous United States, Atmos. Environ., 164, Supplement C, 102–116, 2017.

Ayres, B. R., Allen, H. M., Draper, D. C., Brown, S. S., Wild, R. J., Jimenez, J. L., Day, D. A., Campuzano-Jost, P., Hu, W., de Gouw, J., Koss, A., Cohen, R. C., Duffey, K. C., Romer, P., Baumann, K., Edgerton, E., Takahama, S., Thornton, J. A., Lee, B. H., Lopez-Hilfiker, F. D., Mohr, C., Wennberg, P. O., Nguyen, T. B., Teng, A., Goldstein, A. H., Olson, K., and Fry, J. L.: Organic nitrate aerosol formation via NO_3 + biogenic volatile organic compounds in the southeastern United States, Atmos. Chem. Phys., 15, 13377–13392, https://doi.org/10.5194/acp-15-13377-2015, 2015.

Baker, K. R. and Woody, M. C.: Assessing Model Characterization of Single Source Secondary Pollutant Impacts Using 2013 SENEX Field Study Measurements, Environ. Sci. Technol., 51, 3833–3842, 2017.

Bates, K. H., Crounse, J. D., St. Clair, J. M., Bennett, N. B., Nguyen, T. B., Seinfeld, J. H., Stoltz, B. M., and Wennberg, P. O.: Gas Phase Production and Loss of Isoprene Epoxydiols, J. Phys. Chem. A, 118, 1237–1246, 2014.

Bates, K. H., Nguyen, T. B., Teng, A. P., Crounse, J. D., Kjaergaard, H. G., Stoltz, B. M., Seinfeld, J. H., and Wennberg, P. O.: Production and Fate of C_4 Dihydroxycarbonyl Compounds from Isoprene Oxidation, J. Phys. Chem. A, 120, 106–117, 2016.

Bean, J. K., and Hildebrandt Ruiz, L.: Gas–particle partitioning and hydrolysis of organic nitrates formed from the oxidation of α-pinene in environmental chamber experiments, Atmos. Chem. Phys., 16, 2175–2184, https://doi.org/10.5194/acp-16-2175-2016, 2016.

Blanchard, C. L., Hidy, G. M., Shaw, S., Baumann, K., and Edgerton, E. S.: Effects of emission reductions on organic aerosol in the southeastern United States, Atmos. Chem. Phys., 16, 215–238, https://doi.org/10.5194/acp-16-215-2016, 2016.

Bloomer, B. J., Vinnikov, K. Y., and Dickerson, R. R.: Changes in seasonal and diurnal cycles of ozone and temperature in the eastern U.S., Atmos. Environ., 44, 21–22, 2543–2551, 2010.

Boyd, C. M., Sanchez, J., Xu, L., Eugene, A. J., Nah, T., Tuet, W. Y., Guzman, M. I., and Ng, N. L.: Secondary organic aerosol formation from the β-pinene + NO_3 system: effect of humidity and peroxy radical fate, Atmos. Chem. Phys., 15, 7497–7522, https://doi.org/10.5194/acp-15-7497-2015, 2015.

Boyd, C. M., Nah, T., Xu, L., Berkemeier, T., and Ng, N. L.: Secondary Organic Aerosol (SOA) from Nitrate Radical Oxidation of Monoterpenes: Effects of Temperature, Dilution, and Humidity on Aerosol Formation, Mixing, and Evaporation, Environ. Sci. Technol., 51, 7831–7841, 2017.

Brown-Steiner, B., Hess, P. G., and Lin, M. Y.: On the capabilities and limitations of GCCM simulations of summertime regional air quality: A diagnostic analysis of ozone and temperature simulations in the US using CESM CAM-Chem, Atmos. Environ., 101, 134–148, 2015.

Browne, E. C. and Cohen, R. C.: Effects of biogenic nitrate chemistry on the NO_x lifetime in remote continental regions, Atmos. Chem. Phys., 12, 11917–11932, https://doi.org/10.5194/acp-12-11917-2012, 2012.

Browne, E. C., Wooldridge, P. J., Min, K. E., and Cohen, R. C.: On the role of monoterpene chemistry in the remote continental boundary layer, Atmos. Chem. Phys., 14, 1225–1238, https://doi.org/10.5194/acp-14-1225-2014, 2014.

Camalier, L., Cox, W., and Dolwick, P.: The effects of meteorology on ozone in urban areas and their use in assessing ozone trends, Atmos. Environ., 41, 33, 7127–7137, 2007.

Canty, T. P., Hembeck, L., Vinciguerra, T. P., Anderson, D. C., Goldberg, D. L., Carpenter, S. F., Allen, D. J., Loughner, C. P., Salawitch, R. J., and Dickerson, R. R.: Ozone and NO_x chemistry in the eastern US: evaluation of CMAQ/CB05 with satellite (OMI) data, Atmos. Chem. Phys., 15, 10965–10982, https://doi.org/10.5194/acp-15-10965-2015, 2015.

Cooper, O. R., Gao, R.-S., Tarasick, D., Leblanc, T., and Sweeney, C.: Long-term ozone trends at rural ozone monitoring sites across the United States, 1990–2010, J. Geophys. Res., 117, D22307, https://doi.org/10.1029/2012JD018261, 2012.

Crounse, J. D., Paulot, F., Kjaergaard, H. G., and Wennberg, P. O.: Peroxy radical isomerization in the oxidation of isoprene, Phys. Chem. Chem. Phys., 13, 30, 13607–13613, 2011.

Darer, A. I., Cole-Filipiak, N. C., O'Connor, A. E., and Elrod, M. J.: Formation and Stability of Atmospherically Relevant Isoprene-Derived Organosulfates and Organonitrates, Environ. Sci. Technol., 45, 1895–1902, 2011.

Donner, L. J., Wyman, B. L., Hemler, R. S., Horowitz, L. W., Ming, Y., Zhao, M., Golaz, J.-C., Ginoux, P., Lin, S.-J., Schwarzkopf, M. D., Austin, J., Alaka, G., Cooke, W. F., Delworth, T. L., Freidenreich, S. M., Gordon, C. T., Griffies, S. M., Held, I. M., Hurlin, W. J., Klein, S. A., Knutson, T. R., Langenhorst, A. R., Lee, H.-C., Lin, Y., Magi, B. I., Malyshev, S. L., Milly, P. C. D., Naik, V., Nath, M. J., Pincus, R., Ploshay, J. J., Ramaswamy, V., Seman, C. J., Shevliakova, E., Sirutis, J. J., Stern, W. F., Stouffer, R. J., Wilson, R. J., Winton, M., Wittenberg, A. T., and Zeng, F.: The Dynamical Core, Physical Parameterizations, and Basic Simulation Characteristics of the Atmospheric Component AM3 of the GFDL Global Coupled Model CM3, J. Climate, 24, 3484–3519, 2011.

Edwards, P. M., Aikin, K. C., Dube, W. P., Fry, J. L., Gilman, J. B., de Gouw, J. A., Graus, M. G., Hanisco, T. F., Holloway, J., Hubler, G., Kaiser, J., Keutsch, F. N., Lerner, B. M., Neuman, J. A., Parrish, D. D., Peischl, J., Pollack, I. B., Ravishankara, A. R., Roberts, J. M., Ryerson, T. B., Trainer, M., Veres, P. R., Wolfe, G. M., Warneke, C., and Brown, S. S.: Transition from high- to low-NO_x control of night-time oxidation in the southeastern US, Nat. Geosci., 10, 490–495, 2017.

Fang, Y., Fiore, A. M., Horowitz, L., Levy, H., Hu, Y., and Russell, A.: Sensitivity of the NOy budget over the United States to anthropogenic and lightning NO_x in summer, J. Geophys. Res., 115, D18312, https://doi.org/10.1029/2010JD014079, 2010.

Fehsenfeld, F. C., Ancellet, G., Bates, T. S., Goldstein, A. H., Hardesty, R. M., Honrath, R., Law, K. S., Lewis, A. C., Leaitch, R., McKeen, S., Meagher, J., Parrish, D. D., Pszenny, A. A. P., Russell, P. B., Schlager, H., Seinfeld, J., Talbot, R., and Zbinden, R.: International Consortium for Atmospheric Research on Transport and Transformation (ICARTT): North America to Europe –

Overview of the 2004 summer field study, J. Geophys. Res., 111, D23S01, https://doi.org/10.1029/2006JD007829, 2006.

Fiore, A. M., Horowitz, L. W., Purves, D. W., Levy, H., Evans, M. J., Wang, Y., Li, Q., and Yantosca, R. M.: Evaluating the contribution of changes in isoprene emissions to surface ozone trends over the eastern United States, J. Geophys. Res., 110, D12303, https://doi.org/10.1029/2004JD005485, 2005.

Fiore, A. M., Dentener, F. J., Wild, O., Cuvelier, C., Schultz, M. G., Hess, P., Textor, C., Schulz, M., Doherty, R. M., Horowitz, L. W., MacKenzie, I. A., Sanderson, M. G., Shindell, D. T., Stevenson, D. S., Szopa, S., Van Dingenen, R., Zeng, G., Atherton, C., Bergmann, D., Bey, I., Carmichael, G., Collins, W. J., Duncan, B. N., Faluvegi, G., Folberth, G., Gauss, M., Gong, S., Hauglustaine, D., Holloway, T., Isaksen, I. S. A., Jacob, D. J., Jonson, J. E., Kaminski, J. W., Keating, T. J., Lupu, A., Marmer, E., Montanaro, V., Park, R. J., Pitari, G., Pringle, K. J., Pyle, J. A., Schroeder, S., Vivanco, M. G., Wind, P., Wojcik, G., Wu, S., and Zuber, A.: Multimodel estimates of intercontinental source-receptor relationships for ozone pollution, J. Geophys. Res., 114, D04301, https://doi.org/10.1029/2008JD010816, 2009.

Fischer, E. V., Jacob, D. J., Yantosca, R. M., Sulprizio, M. P., Millet, D. B., Mao, J., Paulot, F., Singh, H. B., Roiger, A., Ries, L., Talbot, R. W., Dzepina, K., and Pandey Deolal, S.: Atmospheric peroxyacetyl nitrate (PAN): a global budget and source attribution, Atmos. Chem. Phys., 14, 2679–2698, https://doi.org/10.5194/acp-14-2679-2014, 2014.

Fisher, J. A., Jacob, D. J., Travis, K. R., Kim, P. S., Marais, E. A., Chan Miller, C., Yu, K., Zhu, L., Yantosca, R. M., Sulprizio, M. P., Mao, J., Wennberg, P. O., Crounse, J. D., Teng, A. P., Nguyen, T. B., St. Clair, J. M., Cohen, R. C., Romer, P., Nault, B. A., Wooldridge, P. J., Jimenez, J. L., Campuzano-Jost, P., Day, D. A., Hu, W., Shepson, P. B., Xiong, F., Blake, D. R., Goldstein, A. H., Misztal, P. K., Hanisco, T. F., Wolfe, G. M., Ryerson, T. B., Wisthaler, A., and Mikoviny, T.: Organic nitrate chemistry and its implications for nitrogen budgets in an isoprene- and monoterpene-rich atmosphere: constraints from aircraft (SEAC4RS) and ground-based (SOAS) observations in the Southeast US, Atmos. Chem. Phys., 16, 5969–5991, https://doi.org/10.5194/acp-16-5969-2016, 2016.

Fry, J. L., Kiendler-Scharr, A., Rollins, A. W., Wooldridge, P. J., Brown, S. S., Fuchs, H., Dubé, W., Mensah, A., dal Maso, M., Tillmann, R., Dorn, H.-P., Brauers, T., and Cohen, R. C.: Organic nitrate and secondary organic aerosol yield from NO_3 oxidation of β-pinene evaluated using a gas-phase kinetics/aerosol partitioning model, Atmos. Chem. Phys., 9, 1431–1449, https://doi.org/10.5194/acp-9-1431-2009, 2009.

Fry, J. L., Draper, D. C., Barsanti, K. C., Smith, J. N., Ortega, J., Winkler, P. M., Lawler, M. J., Brown, S. S., Edwards, P. M., Cohen, R. C., and Lee, L.: Secondary Organic Aerosol Formation and Organic Nitrate Yield from NO_3 Oxidation of Biogenic Hydrocarbons, Environ. Sci. Technol., 48, 11944–11953, 2014.

Granier, C., Bessagnet, B., Bond, T., D'Angiola, A., Denier van der Gon, H., Frost, G. J., Heil, A., Kaiser, J. W., Kinne, S., Klimont, Z., Kloster, S., Lamarque, J.-F., Liousse, C., Masui, T., Meleux, F., Mieville, A., Ohara, T., Raut, J.-C., Riahi, K., Schultz, M. G., Smith, S. J., Thompson, A., van Aardenne, J., van der Werf, G. R., and van Vuuren, D. P.: Evolution of anthropogenic and biomass burning emissions of air pollutants at global and re-gional scales during the 1980–2010 period, Clim. Change, 109, 163–190, 2011.

Grimm, J. W. and Lynch, J. A.: Improved daily precipitation nitrate and ammonium concentration models for the Chesapeake Bay Watershed, Environ. Pollut., 135, 445–455, 2005.

Hardacre, C., Wild, O., and Emberson, L.: An evaluation of ozone dry deposition in global scale chemistry climate models, Atmos. Chem. Phys., 15, 6419–6436, https://doi.org/10.5194/acp-15-6419-2015, 2015.

Henderson, B. H., Pinder, R. W., Crooks, J., Cohen, R. C., Hutzell, W. T., Sarwar, G., Goliff, W. S., Stockwell, W. R., Fahr, A., Mathur, R., Carlton, A. G., and Vizuete, W.: Evaluation of simulated photochemical partitioning of oxidized nitrogen in the upper troposphere, Atmos. Chem. Phys., 11, 275–291, https://doi.org/10.5194/acp-11-275-2011, 2011.

Hidy, G. M., Blanchard, C. L., Baumann, K., Edgerton, E., Tanenbaum, S., Shaw, S., Knipping, E., Tombach, I., Jansen, J., and Walters, J.: Chemical climatology of the southeastern United States, 1999–2013, Atmos. Chem. Phys., 14, 11893–11914, https://doi.org/10.5194/acp-14-11893-2014, 2014.

Hidy, G. M. and Blanchard, C. L.: Precursor reductions and ground-level ozone in the Continental United States, J. Air Waste Manage. Assoc., 65, 1261–1282, https://doi.org/10.1029/97JD03142, 2015.

Horowitz, L. W., Liang, J., Gardner, G. M., and Jacob, D. J.: Export of reactive nitrogen from North America during summertime: Sensitivity to hydrocarbon chemistry, J. Geophys. Res., 103, 13451–13476, 1998.

Horowitz, L. W., Fiore, A. M., Milly, G. P., Cohen, R. C., Perring, A., Wooldridge, P. J., Hess, P. G., Emmons, L. K., and Lamarque, J.-F.: Observational constraints on the chemistry of isoprene nitrates over the eastern United States, J. Geophys. Res., 112, D12S08, https://doi.org/10.1029/2006JD007747, 2007.

Hu, K. S., Darer, A. I., and Elrod, M. J.: Thermodynamics and kinetics of the hydrolysis of atmospherically relevant organonitrates and organosulfates, Atmos. Chem. Phys., 11, 8307–8320, https://doi.org/10.5194/acp-11-8307-2011, 2011.

Hudman, R. C., Jacob, D. J., Cooper, O. R., Evans, M. J., Heald, C. L., Park, R. J., Fehsenfeld, F., Flocke, F., Holloway, J., Hübler, G., Kita, K., Koike, M., Kondo, Y., Neuman, A., Nowak, J., Oltmans, S., Parrish, D., Roberts, J. M., and Ryerson, T.: Ozone production in transpacific Asian pollution plumes and implications for ozone air quality in California, J. Geophys. Res., 109, D23S10, https://doi.org/10.1029/2004JD004974, 2004.

Hudman, R. C., Jacob, D. J., Turquety, S., Leibensperger, E. M., Murray, L. T., Wu, S., Gilliland, A. B., Avery, M., Bertram, T. H., Brune, W., Cohen, R. C., Dibb, J. E., Flocke, F. M., Fried, A., Holloway, J., Neuman, J. A., Orville, R., Perring, A., Ren, X., Sachse, G. W., Singh, H. B., Swanson, A., and Wooldridge, P. J.: Surface and lightning sources of nitrogen oxides over the United States: Magnitudes, chemical evolution, and outflow, J. Geophys. Res., 112, D12S05, https://doi.org/10.1029/2006JD007912, 2007.

Hudman, R. C., Murray, L. T., Jacob, D. J., Turquety, S., Wu, S., Millet, D. B., Avery, M., Goldstein, A. H., and Holloway, J.: North American influence on tropospheric ozone and the effects of recent emission reductions: Constraints from ICARTT observations, J. Geophys. Res., 114, D07302, https://doi.org/10.1029/2008JD010126, 2009.

Hudman, R. C., Moore, N. E., Mebust, A. K., Martin, R. V., Russell, A. R., Valin, L. C., and Cohen, R. C.: Steps towards a mechanistic model of global soil nitric oxide emissions: implementation and space based-constraints, Atmos. Chem. Phys., 12, 7779–7795, https://doi.org/10.5194/acp-12-7779-2012, 2012.

Ito, A., Sillman, S., and Penner, J. E.: Global chemical transport model study of ozone response to changes in chemical kinetics and biogenic volatile organic compounds emissions due to increasing temperatures: Sensitivities to isoprene nitrate chemistry and grid resolution, J. Geophys. Res., 114, D09301, https://doi.org/10.1029/2008JD011254, 2009.

Jacob, D. J. and Winner, D. A.: Effect of climate change on air quality, Atmos. Environ., 43, 1, 51–63, 2009.

Jacobs, M. I., Burke, W. J., and Elrod, M. J.: Kinetics of the reactions of isoprene-derived hydroxynitrates: gas phase epoxide formation and solution phase hydrolysis, Atmos. Chem. Phys., 14, 8933–8946, https://doi.org/10.5194/acp-14-8933-2014, 2014.

Jenkin, M. E., Young, J. C., and Rickard, A. R.: The MCM v3.3.1 degradation scheme for isoprene, Atmos. Chem. Phys., 15, 11433–11459, https://doi.org/10.5194/acp-15-11433-2015, 2015.

Kavassalis, S. and Murphy, J. G.: Understanding ozone-meteorology correlations: a role for dry deposition, Geophys. Res. Lett., 44, 2922–2931, https://doi.org/10.1002/2016GL071791, 2017.

Krotkov, N. A., McLinden, C. A., Li, C., Lamsal, L. N., Celarier, E. A., Marchenko, S. V., Swartz, W. H., Bucsela, E. J., Joiner, J., Duncan, B. N., Boersma, K. F., Veefkind, J. P., Levelt, P. F., Fioletov, V. E., Dickerson, R. R., He, H., Lu, Z., and Streets, D. G.: Aura OMI observations of regional SO_2 and NO_2 pollution changes from 2005 to 2015, Atmos. Chem. Phys., 16, 4605–4629, https://doi.org/10.5194/acp-16-4605-2016, 2016.

Lam, Y. F., Fu, J. S., Wu, S., and Mickley, L. J.: Impacts of future climate change and effects of biogenic emissions on surface ozone and particulate matter concentrations in the United States, Atmos. Chem. Phys., 11, 4789–4806, https://doi.org/10.5194/acp-11-4789-2011, 2011.

Lamarque, J.-F., Kyle, G. P., Meinshausen, M., Riahi, K., Smith, S. J., van Vuuren, D. P., Conley, A. J., and Vitt, F.: Global and regional evolution of short-lived radiatively-active gases and aerosols in the Representative Concentration Pathways, Clim. Change, 109, 191–212, 2011.

Lamsal, L. N., Duncan, B. N., Yoshida, Y., Krotkov, N. A., Pickering, K. E., Streets, D. G., and Lu, Z.: US NO_2 trends (2005–2013): EPA Air Quality System (AQS) data versus improved observations from the Ozone Monitoring Instrument (OMI), Atmos. Environ., 110, 130–143, 2015.

Lee, B. H., Mohr, C., Lopez-Hilfiker, F. D., Lutz, A., Hallquist, M., Lee, L., Romer, P., Cohen, R. C., Iyer, S., Kurtén, T., Hu, W., Day, D. A., Campuzano-Jost, P., Jimenez, J. L., Xu, L., Ng, N. L., Guo, H., Weber, R. J., Wild, R. J., Brown, S. S., Koss, A., de Gouw, J., Olson, K., Goldstein, A. H., Seco, R., Kim, S., McAvey, K., Shepson, P. B., Starn, T., Baumann, K., Edgerton, E. S., Liu, J., Shilling, J. E., Miller, D. O., Brune, W., Schobesberger, S., D'Ambro, E. L., and Thornton, J. A.: Highly functionalized organic nitrates in the southeast United States: Contribution to secondary organic aerosol and reactive nitrogen budgets, P. Natl. Acad. Sci. USA, 113, 1516–1521, 2016.

Lee, L., Teng, A. P., Wennberg, P. O., Crounse, J. D., and Cohen, R. C.: On Rates and Mechanisms of OH and O_3 Reactions with Isoprene-Derived Hydroxy Nitrates, J. Phys. Chem. A, 118, 1622–1637, 2014.

Li, J., Mao, J., Min, K.-E., Washenfelder, R. A., Brown, S. S., Kaiser, J., Keutsch, F. N., Volkamer, R., Wolfe, G. M., Hanisco, T. F., Pollack, I. B., Ryerson, T. B., Graus, M., Gilman, J. B., Lerner, B. M., Warneke, C., de Gouw, J. A., Middlebrook, A. M., Liao, J., Welti, A., Henderson, B. H., McNeill, V. F., Hall, S. R., Ullmann, K., Donner, L. J., Paulot, F., and Horowitz, L. W.: Observational constraints on glyoxal production from isoprene oxidation and its contribution to organic aerosol over the Southeast United States, J. Geophys. Res.-Atmos., 121, 9849–9861, https://doi.org/10.1002/2016JD025331, 2016.

Li, Q., Jacob, D. J., Munger, J. W., Yantosca, R. M., and Parrish, D. D.: Export of NO_y from the North American boundary layer: Reconciling aircraft observations and global model budgets, J. Geophys. Res., 109, D02313, https://doi.org/10.1029/2003JD004086, 2004.

Liang, J., Horowitz, L. W., Jacob, D. J., Wang, Y., Fiore, A. M., Logan, J. A., Gardner, G. M., and Munger, J. W.: Seasonal budgets of reactive nitrogen species and ozone over the United States, and export fluxes to the global atmosphere, J. Geophys. Res., 103, 13435–13450, https://doi.org/10.1029/97JD03126, 1998.

Lin, M., Horowitz, L. W., Payton, R., Fiore, A. M., and Tonnesen, G.: US surface ozone trends and extremes from 1980 to 2014: quantifying the roles of rising Asian emissions, domestic controls, wildfires, and climate, Atmos. Chem. Phys., 17, 2943–2970, https://doi.org/10.5194/acp-17-2943-2017, 2017.

Liu, X., Zhang, Y., Huey, L. G., Yokelson, R. J., Wang, Y., Jimenez, J. L., Campuzano-Jost, P., Beyersdorf, A. J., Blake, D. R., Choi, Y., St. Clair, J. M., Crounse, J. D., Day, D. A., Diskin, G. S., Fried, A., Hall, S. R., Hanisco, T. F., King, L. E., Meinardi, S., Mikoviny, T., Palm, B. B., Peischl, J., Perring, A. E., Pollack, I. B., Ryerson, T. B., Sachse, G., Schwarz, J. P., Simpson, I. J., Tanner, D. J., Thornhill, K. L., Ullmann, K., Weber, R. J., Wennberg, P. O., Wisthaler, A., Wolfe, G. M., and Ziemba, L. D.: Agricultural fires in the southeastern US during SEAC4RS: Emissions of trace gases and particles and evolution of ozone, reactive nitrogen, and organic aerosol, J. Geophys. Res.-Atmos., 121, 7383–7414, https://doi.org/10.1002/2016JD025040, 2016.

Lockwood, A. L., Shepson, P. B., Fiddler, M. N., and Alaghmand, M.: Isoprene nitrates: preparation, separation, identification, yields, and atmospheric chemistry, Atmos. Chem. Phys., 10, 6169–6178, https://doi.org/10.5194/acp-10-6169-2010, 2010.

Lu, Z., Streets, D. G., de Foy, B., Lamsal, L. N., Duncan, B. N., and Xing, J.: Emissions of nitrogen oxides from US urban areas: estimation from Ozone Monitoring Instrument retrievals for 2005–2014, Atmos. Chem. Phys., 15, 10367–10383, https://doi.org/10.5194/acp-15-10367-2015, 2015.

Mao, J., Horowitz, L. W., Naik, V., Fan, S., Liu, J., and Fiore, A. M.: Sensitivity of tropospheric oxidants to biomass burning emissions: implications for radiative forcing, Geophys. Res. Lett., 40, 1241–1246, https://doi.org/10.1002/grl.50210, 2013a.

Mao, J., Paulot, F., Jacob, D. J., Cohen, R. C., Crounse, J. D., Wennberg, P. O., Keller, C. A., Hudman, R. C., Barkley, M. P., and Horowitz, L. W.: Ozone and organic nitrates over the eastern United States: Sensitivity to iso-

prene chemistry, J. Geophys. Res.-Atmos., 118, 11256–11268, https://doi.org/10.1002/jgrd.50817, 2013b.

Metcalfe, S. E., Whyatt, J. D., Nicholson, J. P. G., Derwent, R. G., and Heywood, E.: Issues in model validation: assessing the performance of a regional-scale acid deposition model using measured and modelled data, Atmos. Environ., 39, 587–598, 2005.

Millet, D. B., Jacob, D. J., Boersma, K. F., Fu, T. M., Kurosu, T. P., Chance, K., Heald, C. L., and Guenther, A.: Spatial Distribution of Isoprene Emissions from North America Derived from Dormaldehyde Column Measurements by the OMI Satellite Sensor, J. Geophys. Res., 113, D02307, https://doi.org/10.1029/2007JD008950, 2008.

Miyazaki, K., Eskes, H., Sudo, K., Boersma, K. F., Bowman, K., and Kanaya, Y.: Decadal changes in global surface NO_x emissions from multi-constituent satellite data assimilation, Atmos. Chem. Phys., 17, 807–837, https://doi.org/10.5194/acp-17-807-2017, 2017.

Moxim, W., Levy, H., and Kasibhatla, P.: Simulated global tropospheric PAN: Its transport and impact on NO_x, J. Geophys. Res., 101, 12621–12638, https://doi.org/10.1029/96JD00338, 1996.

Müller, J. F., Peeters, J., and Stavrakou, T.: Fast photolysis of carbonyl nitrates from isoprene, Atmos. Chem. Phys., 14, 2497–2508, https://doi.org/10.5194/acp-14-2497-2014, 2014.

Nah, T., Sanchez, J., Boyd, C. M., and Ng, N. L.: Photochemical Aging of α-pinene and β-pinene Secondary Organic Aerosol formed from Nitrate Radical Oxidation, Environ. Sci. Technol., 50, 222–231, 2016.

Naik, V., Horowitz, L. W., Fiore, A. M., Ginoux, P., Mao, J., Aghedo, A. M., and Levy, H.: Impact of preindustrial to present-day changes in short-lived pollutant emissions on atmospheric composition and climate forcing, J. Geophys. Res.-Atmos., 118, 8086–8110, https://doi.org/10.1002/jgrd.50608, 2013.

Neuman, J. A., Parrish, D. D., Trainer, M., Ryerson, T. B., Holloway, J. S., Nowak, J. B., Swanson, A., Flocke, F., Roberts, J. M., Brown, S. S., Stark, H., Sommariva, R., Stohl, A., Peltier, R., Weber, R., Wollny, A. G., Sueper, D. T., Hubler, G., and Fehsenfeld, F. C.: Reactive nitrogen transport and photochemistry in urban plumes over the North Atlantic Ocean, J. Geophys. Res., 111, D23S54, https://doi.org/10.1029/2005JD007010, 2006.

Ng, N. L., Kwan, A. J., Surratt, J. D., Chan, A. W. H., Chhabra, P. S., Sorooshian, A., Pye, H. O. T., Crounse, J. D., Wennberg, P. O., Flagan, R. C., and Seinfeld, J. H.: Secondary organic aerosol (SOA) formation from reaction of isoprene with nitrate radicals (NO_3), Atmos. Chem. Phys., 8, 4117–4140, https://doi.org/10.5194/acp-8-4117-2008, 2008.

Ng, N. L., Brown, S. S., Archibald, A. T., Atlas, E., Cohen, R. C., Crowley, J. N., Day, D. A., Donahue, N. M., Fry, J. L., Fuchs, H., Griffin, R. J., Guzman, M. I., Herrmann, H., Hodzic, A., Iinuma, Y., Jimenez, J. L., Kiendler-Scharr, A., Lee, B. H., Luecken, D. J., Mao, J., McLaren, R., Mutzel, A., Osthoff, H. D., Ouyang, B., Picquet-Varrault, B., Platt, U., Pye, H. O. T., Rudich, Y., Schwantes, R. H., Shiraiwa, M., Stutz, J., Thornton, J. A., Tilgner, A., Williams, B. J., and Zaveri, R. A.: Nitrate radicals and biogenic volatile organic compounds: oxidation, mechanisms, and organic aerosol, Atmos. Chem. Phys., 17, 2103–2162, https://doi.org/10.5194/acp-17-2103-2017, 2017.

Nguyen, T. B., Crounse, J. D., Teng, A. P., St. Clair, J. M., Paulot, F., Wolfe, G. M., and Wennberg, P. O.: Rapid deposition of oxidized biogenic compounds to a temperate forest, P. Natl. Acad. Sci. USA, 112, E392–E401, 2015.

Nozière, B., Barnes, I., and Becker, K. H.: Product study and mechanisms of the reactions of α-pinene and of pinonaldehyde with OH radicals, J. Geophys. Res., 104, 23645–23656, https://doi.org/10.1029/1999JD900778, 1999.

Ott, L. E., Pickering, K. E., Stenchikov, G. L., Allen, D. J., DeCaria, A. J., Ridley, B., Lin, R.-F., Lang, S., and Tao, W.-K.: Production of lightning NO_x and its vertical distribution calculated from three-dimensional cloud-scale chemical transport model simulations, J. Geophys. Res., 115, D04301, https://doi.org/10.1029/2009JD011880, 2010.

Parrish, D. D., Ryerson, T. B., Holloway, J. S., Neuman, J. A., Roberts, J. M., Williams, J., Stroud, C. A., Frost, G. J., Trainer, M., Hübler, G., Fehsenfeld, F. C., Flocke, F., and Weinheimer, A. J.: Fraction and composition of NO_y transported in air masses lofted from the North American continental boundary layer, J. Geophys. Res., 109, D09302, https://doi.org/10.1029/2003JD004226, 2004.

Paulot, F., Crounse, J. D., Kjaergaard, H. G., Kroll, J. H., Seinfeld, J. H., and Wennberg, P. O.: Isoprene photooxidation: new insights into the production of acids and organic nitrates, Atmos. Chem. Phys., 9, 1479–1501, https://doi.org/10.5194/acp-9-1479-2009, 2009.

Paulot, F., Henze, D. K., and Wennberg, P. O.: Impact of the isoprene photochemical cascade on tropical ozone, Atmos. Chem. Phys., 12, 1307–1325, https://doi.org/10.5194/acp-12-1307-2012, 2012.

Paulot, F., Jacob, D. J., Pinder, R. W., Bash, J. O., Travis, K., and Henze, D. K.: Ammonia emissions in the United States, European Union, and China derived by high-resolution inversion of ammonium wet deposition data: Interpretation with a new agricultural emissions inventory (MASAGE_NH3), J. Geophys. Res.-Atmos., 119, 4343–4364, https://doi.org/10.1002/2013JD021130, 2014.

Paulot, F., Ginoux, P., Cooke, W. F., Donner, L. J., Fan, S., Lin, M.-Y., Mao, J., Naik, V., and Horowitz, L. W.: Sensitivity of nitrate aerosols to ammonia emissions and to nitrate chemistry: implications for present and future nitrate optical depth, Atmos. Chem. Phys., 16, 1459–1477, https://doi.org/10.5194/acp-16-1459-2016, 2016.

Peeters, J., Müller, J.-F., Stavrakou, T., and Nguyen, V. S.: Hydroxyl Radical Recycling in Isoprene Oxidation Driven by Hydrogen Bonding and Hydrogen Tunneling: The Upgraded LIM1 Mechanism, J. Phys. Chem. A, 118, 8625–8643, 2014.

Perring, A. E., Bertram, T. H., Wooldridge, P. J., Fried, A., Heikes, B. G., Dibb, J., Crounse, J. D., Wennberg, P. O., Blake, N. J., Blake, D. R., Brune, W. H., Singh, H. B., and Cohen, R. C.: Airborne observations of total $RONO_2$: new constraints on the yield and lifetime of isoprene nitrates, Atmos. Chem. Phys., 9, 1451–1463, https://doi.org/10.5194/acp-9-1451-2009, 2009.

Perring, A. E., Pusede, S. E., and Cohen, R. C.: An Observational Perspective on the Atmospheric Impacts of Alkyl and Multifunctional Nitrates on Ozone and Secondary Organic Aerosol, Chem. Rev., 113, 5848–5870, 2013.

Philip, S., Martin, R. V., and Keller, C. A.: Sensitivity of chemistry-transport model simulations to the duration of chemical and transport operators: a case study with GEOS-Chem v10-01,

Geosci. Model Dev., 9, 1683–1695, https://doi.org/10.5194/gmd-9-1683-2016, 2016.

Pickering, K. E., Wang, Y., Tao, W. K., Price, C., and Müller, J. F.: Vertical distributions of lightning NO_x for use in regional and global chemical transport models, J. Geophys. Res., 103, 31203–31216, https://doi.org/10.1029/98JD02651, 1998.

Pierce, R. B., Schaack, T., Al-Saadi, J. A., Fairlie, T. D., Kittaka, C., Lingenfelser, G., Natarajan, M., Olson, J., Soja, A., Zapotocny, T., Lenzen, A., Stobie, J., Johnson, D., Avery, M. A., Sachse, G. W., Thompson, A., Cohen, R., Dibb, J. E., Crawford, J., Rault, D., Martin, R., Szykman, J., and Fishman, J.: Chemical data assimilation estimates of continental US ozone and nitrogen budgets during the Intercontinental Chemical Transport Experiment–North America, J. Geophys. Res., 112, D12S21, https://doi.org/10.1029/2006JD007722, 2007.

Pollack, I. B., Ryerson, T. B., Trainer, M., Neuman, J., Roberts, J. M., and Parrish, D. D.: Trends in ozone, its precursors, and related secondary oxidation products in Los Angeles, California: A synthesis of measurements from 1960 to 2010, J. Geophys. Res., 118, 5893–5911, https://doi.org/10.1002/jgrd.50472, 2013.

Praske, E., Crounse, J. D., Bates, K. H., Kurtén, T., Kjaergaard, H. G., and Wennberg, P. O.: Atmospheric Fate of Methyl Vinyl Ketone: Peroxy Radical Reactions with NO and HO_2, J. Phys. Chem. A, 119, 4562–4572, 2015.

Pye, H. O. T., Luecken, D. J., Xu, L., Boyd, C. M., Ng, N. L., Baker, K. R., Ayres, B. R., Bash, J. O., Baumann, K., Carter, W. P. L., Edgerton, E., Fry, J. L., Hutzell, W. T., Schwede, D. B., and Shepson, P. B.: Modeling the Current and Future Roles of Particulate Organic Nitrates in the Southeastern United States, Environ. Sci. Technol., 49, 14195–14203, 2015.

Rieder, H. E., Fiore, A. M., Horowitz, L. W., and Naik, V.: Projecting policy-relevant metrics for high summertime ozone pollution events over the eastern United States due to climate and emission changes during the 21st century, J. Geophys. Res., 120, 784–800, https://doi.org/10.1002/2014JD022303, 2015.

Rindelaub, J. D., McAvey, K. M., and Shepson, P. B.: The photochemical production of organic nitrates from α-pinene and loss via acid-dependent particle phase hydrolysis, Atmos. Environ., 100, 193–201, 2015.

Rindelaub, J. D., Borca, C. H., Hostetler, M. A., Slade, J. H., Lipton, M. A., Slipchenko, L. V., and Shepson, P. B.: The acid-catalyzed hydrolysis of an a-pinene-derived organic nitrate: kinetics, products, reaction mechanisms, and atmospheric impact, Atmos. Chem. Phys., 16, 15425–15432, https://doi.org/10.5194/acp-16-15425-2016, 2016.

Rollins, A. W., Kiendler-Scharr, A., Fry, J. L., Brauers, T., Brown, S. S., Dorn, H.-P., Dubé, W. P., Fuchs, H., Mensah, A., Mentel, T. F., Rohrer, F., Tillmann, R., Wegener, R., Wooldridge, P. J., and Cohen, R. C.: Isoprene oxidation by nitrate radical: alkyl nitrate and secondary organic aerosol yields, Atmos. Chem. Phys., 9, 6685–6703, https://doi.org/10.5194/acp-9-6685-2009, 2009.

Rollins, A. W., Smith, J. D., Wilson, K. R., and Cohen, R. C.: Real Time In Situ Detection of Organic Nitrates in Atmospheric Aerosols, Environ. Sci. Technol., 44, 14, 5540–5545, 2010.

Romer, P. S., Duffey, K. C., Wooldridge, P. J., Allen, H. M., Ayres, B. R., Brown, S. S., Brune, W. H., Crounse, J. D., de Gouw, J., Draper, D. C., Feiner, P. A., Fry, J. L., Goldstein, A. H., Koss, A., Misztal, P. K., Nguyen, T. B., Olson, K., Teng, A. P., Wennberg, P. O., Wild, R. J., Zhang, L., and Cohen, R. C.: The

lifetime of nitrogen oxides in an isoprene-dominated forest, Atmos. Chem. Phys., 16, 7623–7637, https://doi.org/10.5194/acp-16-7623-2016, 2016.

Russell, A. R., Valin, L. C., and Cohen, R. C.: Trends in OMI NO_2 observations over the United States: effects of emission control technology and the economic recession, Atmos. Chem. Phys., 12, 12197–12209, https://doi.org/10.5194/acp-12-12197-2012, 2012.

Sanderson, M. G., Dentener, F. J., Fiore, A. M., Cuvelier, C., Keating, T. J., Zuber, A., Atherton, C. S., Bergmann, D. J., Diehl, T., Doherty, R. M., Duncan, B. N., Hess, P., Horowitz, L. W., Jacob, D. J., Jonson, J. E., Kaminski, J. W., Lupu, A., MacKenzie, I. A., Mancini, E., Marmer, E., Park, R., Pitari, G., Prather, M. J., Pringle, K. J., Schroeder, S., Schultz, M. G., Shindell, D. T., Szopa, S., Wild, O., and Wind, P.: A multi-model study of the hemispheric transport and deposition of oxidised nitrogen, Geophys. Res. Lett., 35, L17815, https://doi.org/10.1029/2008GL035389, 2008.

Sato, K.: Detection of nitrooxypolyols in secondary organic aerosol formed from the photooxidation of conjugated dienes under high-NO_x conditions, Atmos. Environ., 42, 6851–6861, 2008.

Schwantes, R. H., Teng, A. P., Nguyen, T. B., Coggon, M. M., Crounse, J. D., St. Clair, J. M., Zhang, X., Schilling, K. A., Seinfeld, J. H., and Wennberg, P. O.: Isoprene NO_3 Oxidation Products from the RO_2 + HO_2 Pathway, J. Phys. Chem. A, 119, 10158–10171, 2015.

Sillman, S.: Ozone production efficiency and loss of NO_x in power plant plumes: Photochemical model and interpretation of measurements in Tennessee, J. Geophys. Res., 105, 9189–9202, https://doi.org/10.1029/1999JD901014, 2000.

Simon, H., Reff, A., Wells, B., Xing, J., and Frank, N.: Ozone Trends Across the United States over a Period of Decreasing NO_x and VOC Emissions, Environ. Sci. Technol., 49, 186–195, 2015.

Singh, H. B., Brune, W. H., Crawford, J. H., Jacob, D. J., and Russell, P. B.: Overview of the summer 2004 Intercontinental Chemical Transport Experiment–North America (INTEX-A), J. Geophys. Res., 111, D24S01, https://doi.org/10.1029/2006JD007905, 2006.

Singh, H. B., Salas, L., Herlth, D., Kolyer, R., Czech, E., Avery, M., Crawford, J. H., Pierce, R. B., Sachse, G. W., Blake, D. R., Cohen, R. C., Bertram, T. H., Perring, A., Wooldridge, P. J., Dibb, J., Huey, G., Hudman, R. C., Turquety, S., Emmons, L. K., Flocke, F., Tang, Y., Carmichael, G. R., and Horowitz, L. W.: Reactive nitrogen distribution and partitioning in the North American troposphere and lowermost stratosphere, J. Geophys. Res., 112, D12S04, https://doi.org/10.1029/2006JD007664, 2007.

Spittler, M., Barnes, I., Bejan, I., Brockmann, K. J., Benter, T., and Wirtz, K.: Reactions of NO_3 radicals with limonene and α-pinene: Product and SOA formation, Atmos. Environ., 40, 116–127, 2006.

St. Clair, J. M., Rivera-Rios, J. C., Crounse, J. D., Knap, H. C., Bates, K. H., Teng, A. P., Jørgensen, S., Kjaergaard, H. G., Keutsch, F. N., and Wennberg, P. O.: Kinetics and Products of the Reaction of the First-Generation Isoprene Hydroxy Hydroperoxide (ISOPOOH) with OH, J. Phys. Chem. A, 120, 1441–1451, 2016.

Steiner, A. L., Davis, A. J., Sillman, S., Owen, R. C., Michalak, A. M., and Fiore, A. M.: Observed suppression of ozone formation

at extremely high temperatures due to chemical and biophysical feedbacks, P. Natl. Acad. Sci. USA, 107, 19685–19690, 2010.

Stoeckenius, T. E., Hogrefe, C., Zagunis, J., Sturtz, T. M., Wells, B., and Sakulyanontvittaya, T.: A comparison between 2010 and 2006 air quality and meteorological conditions, and emissions and boundary conditions used in simulations of the AQMEII-2 North American domain, Atmos. Environ., 115, 389–403, 2015.

Stohl, A., Trainer, M., Ryerson, T. B., Holloway, J. S., and Parrish, D. D.: Export of NO_y from the North American boundary layer during 1996 and 1997 North Atlantic Regional Experiments, J. Geophys. Res., 107, https://doi.org/10.1029/2001JD000519, 2002.

Strode, S. A., Rodriguez, J. M., Logan, J. A., Cooper, O. R., Witte, J. C., Lamsal, L. N., Damon, M., Van Aartsen, B., Steenrod, S. D., and Strahan, S. E.: Trends and variability in surface ozone over the United States, J. Geophys. Res.-Atmos., 120, 9020–9042, https://doi.org/10.1002/2014JD022784, 2015.

Szmigielski, R., Vermeylen, R., Dommen, J., Metzger, A., Maenhaut, W., Baltensperger, U., and Claeys, M.: The acid effect in the formation of 2-methyltetrols from the photooxidation of isoprene in the presence of NO_x, Atmos. Res., 98, 183–189, 2010.

Tawfik, A. B. and Steiner, A. L.: A proposed physical mechanism for ozone-meteorology correlations using land–atmosphere coupling regimes, Atmos. Environ., 72, 50–59, 2013.

Teng, A. P., Crounse, J. D., Lee, L., St. Clair, J. M., Cohen, R. C., and Wennberg, P. O.: Hydroxy nitrate production in the OH-initiated oxidation of alkenes, Atmos. Chem. Phys., 15, 4297–4316, https://doi.org/10.5194/acp-15-4297-2015, 2015.

Tong, D. Q., Lamsal, L., Pan, L., Ding, C., Kim, H., Lee, P., Chai, T., Pickering, K. E., and Stajner, I.: Long-term NO_x trends over large cities in the United States during the great recession: Comparison of satellite retrievals, ground observations, and emission inventories, Atmos. Environ., 107, 70–84, 2015.

Toon, O. B., Maring, H., Dibb, J., Ferrare, R., Jacob, D. J., Jensen, E. J., Luo, Z. J., Mace, G. G., Pan, L. L., Pfister, L., Rosenlof, K. H., Redemann, J., Reid, J. S., Singh, H. B., Thompson, A. M., Yokelson, R., Minnis, P., Chen, G., Jucks, K. W., and Pszenny, A.: Planning, implementation and scientific goals of the Studies of Emissions and Atmospheric Composition, Clouds and Climate Coupling by Regional Surveys (SEAC4RS) field mission, J. Geophys. Res., 121, 4967–5009, https://doi.org/10.1002/2015JD024297, 2016.

Tost, H., Jöckel, P., Kerkweg, A., Pozzer, A., Sander, R., and Lelieveld, J.: Global cloud and precipitation chemistry and wet deposition: tropospheric model simulations with ECHAM5/MESSy1, Atmos. Chem. Phys., 7, 2733–2757, https://doi.org/10.5194/acp-7-2733-2007, 2007.

Trainer, M., Parrish, D. D., Goldan, P. D., Roberts, J., and Fehsenfeld, F. C.: Review of observation-based analysis of the regional factors influencing ozone concentrations, Atmos. Environ., 34, 2045–2061, 2000.

Travis, K. R., Jacob, D. J., Fisher, J. A., Kim, P. S., Marais, E. A., Zhu, L., Yu, K., Miller, C. C., Yantosca, R. M., Sulprizio, M. P., Thompson, A. M., Wennberg, P. O., Crounse, J. D., St. Clair, J. M., Cohen, R. C., Laughner, J. L., Dibb, J. E., Hall, S. R., Ullmann, K., Wolfe, G. M., Pollack, I. B., Peischl, J., Neuman, J. A., and Zhou, X.: Why do models overestimate surface ozone in the Southeast United States?, Atmos. Chem. Phys., 16, 13561–13577, https://doi.org/10.5194/acp-16-13561-2016, 2016.

Val Martin, M., Heald, C. L., and Arnold, S. R.: Coupling dry deposition to vegetation phenology in the Community Earth System Model: Implications for the simulation of surface O_3, Geophys. Res. Lett., 41, 2988–2996, https://doi.org/10.1002/2014GL059651, 2014.

Warneke, C., Trainer, M., de Gouw, J. A., Parrish, D. D., Fahey, D. W., Ravishankara, A. R., Middlebrook, A. M., Brock, C. A., Roberts, J. M., Brown, S. S., Neuman, J. A., Lerner, B. M., Lack, D., Law, D., Hübler, G., Pollack, I., Sjostedt, S., Ryerson, T. B., Gilman, J. B., Liao, J., Holloway, J., Peischl, J., Nowak, J. B., Aikin, K. C., Min, K. E., Washenfelder, R. A., Graus, M. G., Richardson, M., Markovic, M. Z., Wagner, N. L., Welti, A., Veres, P. R., Edwards, P., Schwarz, J. P., Gordon, T., Dube, W. P., McKeen, S. A., Brioude, J., Ahmadov, R., Bougiatioti, A., Lin, J. J., Nenes, A., Wolfe, G. M., Hanisco, T. F., Lee, B. H., Lopez-Hilfiker, F. D., Thornton, J. A., Keutsch, F. N., Kaiser, J., Mao, J., and Hatch, C. D.: Instrumentation and measurement strategy for the NOAA SENEX aircraft campaign as part of the Southeast Atmosphere Study 2013, Atmos. Meas. Tech., 9, 3063–3093, https://doi.org/10.5194/amt-9-3063-2016, 2016.

Wolfe, G. M., Hanisco, T. F., Arkinson, H. L., Bui, T. P., Crounse, J. D., Dean-Day, J., Goldstein, A., Guenther, A., Hall, S. R., Huey, G., Jacob, D. J., Karl, T., Kim, P. S., Liu, X., Marvin, M. R., Mikoviny, T., Misztal, P. K., Nguyen, T. B., Peischl, J., Pollack, I., Ryerson, T., St. Clair, J. M., Teng, A., Travis, K. R., Ullmann, K., Wennberg, P. O., and Wisthaler, A.: Quantifying sources and sinks of reactive gases in the lower atmosphere using airborne flux observations, Geophys. Res. Lett., 42, 8231–8240, 2015.

Wu, S., Mickley, L. J., Jacob, D. J., Rind, D., and Streets, D. G.: Effects of 2000–2050 changes in climate and emissions on global tropospheric ozone and the policy-relevant background surface ozone in the United States, J. Geophys. Res., 113, D18312, https://doi.org/10.1029/2007JD009639, 2008.

Xing, J., Mathur, R., Pleim, J., Hogrefe, C., Gan, C. M., Wong, D. C., Wei, C., Gilliam, R., and Pouliot, G.: Observations and modeling of air quality trends over 1990–2010 across the Northern Hemisphere: China, the United States and Europe, Atmos. Chem. Phys., 15, 2723–2747, https://doi.org/10.5194/acp-15-2723-2015, 2015.

Xiong, F., McAvey, K. M., Pratt, K. A., Groff, C. J., Hostetler, M. A., Lipton, M. A., Starn, T. K., Seeley, J. V., Bertman, S. B., Teng, A. P., Crounse, J. D., Nguyen, T. B., Wennberg, P. O., Misztal, P. K., Goldstein, A. H., Guenther, A. B., Koss, A. R., Olson, K. F., de Gouw, J. A., Baumann, K., Edgerton, E. S., Feiner, P. A., Zhang, L., Miller, D. O., Brune, W. H., and Shepson, P. B.: Observation of isoprene hydroxynitrates in the southeastern United States and implications for the fate of NO_x, Atmos. Chem. Phys., 15, 11257–11272, https://doi.org/10.5194/acp-15-11257-2015, 2015.

Xiong, F., Borca, C. H., Slipchenko, L. V., and Shepson, P. B.: Photochemical degradation of isoprene-derived 4,1-nitrooxy enal, Atmos. Chem. Phys., 16, 5595–5610, https://doi.org/10.5194/acp-16-5595-2016, 2016.

Xu, L., Suresh, S., Guo, H., Weber, R. J., and Ng, N. L.: Aerosol characterization over the southeastern United States using high-resolution aerosol mass spectrometry: spatial and seasonal variation of aerosol composition and sources with a focus on organic nitrates, Atmos. Chem. Phys., 15, 7307–7336, https://doi.org/10.5194/acp-15-7307-2015, 2015.

Yahya, K., Wang, K., Campbell, P., Glotfelty, T., He, J., and Zhang, Y.: Decadal evaluation of regional climate, air quality, and their interactions over the continental US and their interactions using WRF/Chem version 3.6.1, Geosci. Model Dev., 9, 671–695, https://doi.org/10.5194/gmd-9-671-2016, 2016.

Yienger, J. J. and Levy, H.: Empirical model of global soil-biogenic NO_x emissions, J. Geophys. Res., 100, 11447–11464, https://doi.org/10.1029/95JD00370, 1995.

Yu, K., Jacob, D. J., Fisher, J. A., Kim, P. S., Marais, E. A., Miller, C. C., Travis, K. R., Zhu, L., Yantosca, R. M., Sulprizio, M. P., Cohen, R. C., Dibb, J. E., Fried, A., Mikoviny, T., Ryerson, T. B., Wennberg, P. O., and Wisthaler, A.: Sensitivity to grid resolution in the ability of a chemical transport model to simulate observed oxidant chemistry under high-isoprene conditions, Atmos. Chem. Phys., 16, 4369–4378, https://doi.org/10.5194/acp-16-4369-2016, 2016.